

copy # 11-38271

NASA CR-145097

N 77-14614

FINAL REPORT
PHASE I,
URBAN AIR QUALITY ESTIMATION STUDY

By

John M. Diamante, Thomas S. Englar, Jr.,
and Andrew H. Jazwinski

REPRODUCIBLE COPY
(FACILITY CASEFILE COPY)

Report No. BTS TR-76-28

Prepared under Contract No. NAS 1-13764

By

BUSINESS AND TECHNOLOGICAL SYSTEMS, INC.

Aerospace Building, Suite 440

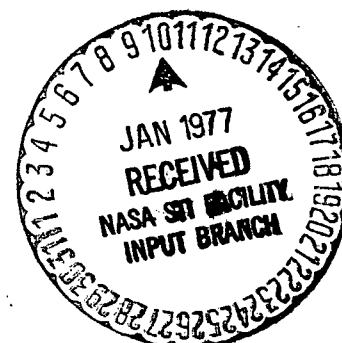
10210 Greenbelt Road

Seabrook, Maryland 20801

For

NASA

National Aeronautics and
Space Administration



January 1976

FOREWORD

This report describes the work performed by Business and Technological Systems, Inc. under the first phase of Contract No. NAS 1-13764 with the NASA/Langley Research Center. The report describes the development of various levels of mathematical models required for the application of formal estimation theory techniques to the problem of urban air quality estimation for elevated point sources.

ACKNOWLEDGEMENTS

The authors wish to acknowledge the contributions provided to the work reported here by Dr. G. Louis Smith, Technical Monitor, Mr. Richard N. Green, Mr. James Kibler, Mr. John T. Suttles, Mr. George R. Young, all of NASA Langley Research Center. The ideas and valuable discussion interchanged during periodic meetings held between the authors and the above NASA/Langley technical staff has influenced all phases of this effort.

TABLE OF CONTENTS

	<u>PAGE</u>
FOREWORD.....	i
ACKNOWLEDGEMENTS.....	ii
SUMMARY.....	iv
LIST OF SYMBOLS.....	v
I. INTRODUCTION.....	1
II. PROPERTIES OF REAL PLUMES FROM ELEVATED POINT SOURCES RELATED TO THE PROBLEMS OF DISPERSION AND MEASUREMENT MODELING.....	7
III. INSTANTANEOUS AND TIME AVERAGED POINT SOURCE PLUME MODELS.....	15
IV. DISPERSION PARAMETER MODELS AND A PRIORI INFORMATION.....	27
V. SIMPLIFIED REMOTE AND IN SITU MEASUREMENT MODELS.....	51
VI. CONCLUSIONS.....	73
VII. REFERENCES.....	75
APPENDIX A - DEVELOPMENT OF INSTANTANEOUS PLUME CENTERLINE MODEL.....	A1
APPENDIX B - CONSIDERATIONS OF THE GAUSSIAN NATURE OF PLUME PARAMETERS.....	B1

SUMMARY

Major research results in the contract year have included: (A) The fluctuating plume model of Gifford (1959) has been extended by inclusion of an effective stack height, application of a surface reflection condition at the ground and including influences of a mixing layer to provide an expression for the instantaneous concentration X due to an elevated point source (e.g. a smoke stack). This model has the important property that the formal calculation of its statistical expected value is identified with the expression for the mean plume concentration \bar{X} based on the Gaussian point source plume model given by Turner (1970). The Turner model is a major component of many operational steady-state diffusion models. (B) Formal mathematical relationships between the basic parameters of the fluctuating and steady-state plume models have also been formulated, providing a theoretical basis for relating instantaneous and time-averaged plume measurements. (C) In order to employ measurements with the fluctuating plume model in an estimation procedure, similar to that given by Smith, Young and Green (1974a,b) for the steady-state plume model, individual models for each of the parameters appearing in both plume equations and models of the various measurement types have been developed. The models include the stochastic properties of the instantaneous fluctuating plume. The model development provides a basis for the systematic incorporation of *a priori* dispersion knowledge and associated uncertainties with different measurement types using estimation theory techniques to provide air quality estimates on self-consistent time scales. (D) Measurement and sensitivity models have been developed for measurement types having radically different time and space averaging. Measurement types include fast response spatially integrated values and fast response and time-averaged point measurements. The measurement model development includes the categories of fast response remote based types from satellite and aircraft platforms, time-averaged or instantaneous ground based *in situ* types, instantaneous *in situ* measurements from airborne or other mobile platforms, etc. The formalism for dealing with measurement types which include both time and space averaging (i.e. slow response spatially integrated measurements) has also been outlined.

LIST OF SYMBOLS

<u>SYMBOL</u>	<u>DESCRIPTION</u>
a	Exponent in the relation for the crosswind standard deviation σ_θ as a function of averaging time δT .
A_0	Area of the circular footprint in the remote measurement model.
C	Wavelength to amplitude ratio for fluctuations of the instantaneous plume.
D	Average instantaneous plume width.
D_f	Diameter of the footprint in the remote measurement model.
D_y or $D_y(x,t)$	Crosswind displacement, relative to the mean wind axis (average plume line), of the instantaneous plume centerline (or mass center of the instantaneous puff, as the case may be).
D_z or $D_z(x,t)$	Vertical displacement, relative to the mean wind axis of the instantaneous plume centerline (or mass center of the instantaneous puff, as the case may be).
D_η or $D_\eta(x,t)$	D_y and/or D_z , as the case may be.
$\overline{D_y^2}$ or $\overline{D_y^2}(x)$	Variance in the crosswind direction of the frequency distribution of the fluctuating plume centerline displacement from the mean plume axis, i.e. variance of the frequency distribution for D_y .
$\overline{D_z^2}$ or $\overline{D_z^2}(x)$	Variance in the vertical direction of the frequency distribution of the fluctuating plume centerline displacement from the mean plume axis, i.e. the variance of the frequency distribution for D_z .
$\overline{D_\eta^2}$ or $\overline{D_\eta^2}(x)$	$\overline{D_y^2}$ and/or $\overline{D_z^2}$, as the case may be.

LIST OF SYMBOLS (Cont.)

<u>SYMBOL</u>	<u>DESCRIPTION</u>
\overline{D}_{y0}^2	Coefficient in the $\overline{D}_y^2(x)$ equation, corresponding to the value of $\overline{D}_y^2(x)$ at x equal to one meter.
\overline{D}_{z0}^2	Coefficient in the $\overline{D}_z^2(x)$ equation, corresponding to the value of $\overline{D}_z^2(x)$ at x equal to one meter (in the absence of mixing layer effects).
$\overline{D}_{y\infty}^2$	Limiting value of $\overline{D}_y^2(x)$.
$\overline{D}_{z\infty}^2$	Limiting value of $\overline{D}_z^2(x)$, in the absence of mixing layer effects.
\overline{D}_{zL}^2	Limiting value of $\overline{D}_z^2(x)$ in the presence of mixing layer effects.
e	Base of natural logarithms ($\approx 2.71828\dots$).
$E\{\cdot\}$	Expected value or mean operator.
$\text{erf}\{\cdot\}$	Error function: $\text{erf}\{\cdot\} = (2/\sqrt{\pi}) \int_0^{\{\cdot\}} e^{-\xi^2} d\xi$
$\exp\{\cdot\}$	Exponential operator, i.e. $\exp\{\cdot\} \equiv e^{\{\cdot\}}$
$f(\cdot)$	Material distribution function.
f_y or $f_y(x)$	Amplitude function in the $D_y(x,t)$ relation, set equal to the standard deviation of the frequency distribution for D_y , i.e. $f_y \equiv \sqrt{\overline{D}_y^2}$.
f_z or $f_z(x)$	Amplitude function in the $D_z(x,t)$ relation, set equal to the standard deviation of the frequency distribution for D_z , i.e. $f_z \equiv \sqrt{\overline{D}_z^2}$.
f_η or $f_\eta(x)$	f_y and/or f_z , as the case may be.

LIST OF SYMBOLS (Cont.)

<u>SYMBOL</u>	<u>DESCRIPTION</u>
$f_{\eta}(\infty)$	Limiting value of f_{η} .
$f_{D_y}(y)$	Frequency function (probability density) for D_y .
$f_{D_z}(z)$	Frequency function for D_z .
$f_{D_{\eta}}(n)$	$f_{D_y}(y)$ and/or $f_{D_z}(z)$, as the case may be.
$f_{D_{\eta}}/f_{\eta}$	Frequency function for D_{η}/f_{η} .
$f_{\gamma_{1_y}}$	Probability density function for γ_{1_y} .
$f_{\gamma_{1_z}}$	Probability density function for γ_{1_z} .
$f_{\gamma_{2_y}}$	Probability density function for γ_{2_y} .
$f_{\gamma_{2_z}}$	Probability density function for γ_{2_z} .
$f_{\gamma_{1_{\eta}}}$	$f_{\gamma_{1_y}}$ and/or $f_{\gamma_{1_z}}$, as the case may be.
$f_{\gamma_{2_{\eta}}}$	$f_{\gamma_{2_y}}$ and/or $f_{\gamma_{2_z}}$, as the case may be.
$g_{\eta}(x,t)$	Wavelength function in the $D_{\eta}(x,t)$ model.
$g_1(D_y)$	The frequency function for D_y , $g_1(D_y) \equiv f_{D_y}(y)$.
$g_2(D_z)$	The frequency function for D_z , $g_2(D_z) \equiv f_{D_z}(z)$.
h_T	Height of the tropopause.
H	Effective stack height (effective vertical position) of the elevated point source.
H_0	Physical stack height.

LIST OF SYMBOLS (Cont.)

<u>SYMBOL</u>	<u>DESCRIPTION</u>
$I(x)$	Interpolation function based on the hyperbolic tangent.
$I_t(\delta T)$	Interpolation function based on the hyperbolic tangent.
$J(z)$	Altitude dependent weighting function for remote measurement model.
k_i^0	Gain of instrument at position \vec{r}_i in slow response or time-averaged <i>in situ</i> measurement model.
k_i^1	Bias of instrument at position \vec{r}_i in slow response or time-averaged <i>in situ</i> measurement model.
$K(\sigma)$	"Clipping" function employed to provide a smooth approach to a limiting value for all averaging times δT in the $\sigma_z^{-2}(x, \delta T)$ model when mixing ceiling effects are present.
K_0	Instrument gain in remote measurement model.
K_1	Instrument bias in remote measurement model.
K_i^0	Gain of instrument at position \vec{r}_i in fast response <i>in situ</i> measurement model.
K_i^1	Bias of instrument at position \vec{r}_i in fast response <i>in situ</i> measurement model.
ℓ	Characteristic eddy dimension.
L	Characteristic horizontal scale length, usually downwind distance from the source unless noted otherwise.
L_0	Specific downwind distance.

LIST OF SYMBOLS (Cont.)

<u>SYMBOL</u>	<u>DESCRIPTION</u>
L'	The approximate downwind distance corresponding to an averaging time $\delta t(L')$ (required to just average out the eddy fluctuations) that just equals some fixed instrument averaging time $\delta T'$.
L	Mixing height.
\dot{M}	Remote measurement data rate (measurements per second).
p	Exponent in the power law relation for σ_y .
P	Exponent in the $\overline{D_y^2}(x)$ relation.
Peak(\bar{X})	The peak value of the concentration \bar{X} (on the plume axis).
$q(x)$	Exponent in σ_z relation.
q_0	Constant in $q(x)$ expression.
q'	Coefficient in $q(x)$ expression.
q_{1_n}	Variance of white noise v_{1_n} .
q_{2_n}	Variance of white noise v_{2_n} .
q_{3_n}	Variance of white noise v_{3_n} .
q_{4_n}	Variance of white noise v_{4_n} .
q_{i_n}	q_{1_n} , q_{2_n} , q_{3_n} , and/or q_{4_n} ($i=1,2,3,4$).
Q	Source strength (average pollutant mass production rate, mass/time).

LIST OF SYMBOLS (Cont.)

<u>SYMBOL</u>	<u>DESCRIPTION</u>
Q or $Q(x)$	Exponent in $\overline{D_z^2}(x)$ relation.
Q_0	Constant in $Q(x)$ expression.
Q'	Coefficient in $Q(x)$ expression.
Q_d	The total amount of pollutant in a disk (puff).
\vec{r}_i	Position of <i>in situ</i> instrument, $\vec{r}_i \equiv (x_i, y_i, z_i)$.
r_{ih}	Horizontal resolution of the remote measurement.
s or $s(\delta T)$	Exponent of the power law relation between \overline{X} and $\overline{\overline{X}}$, σ_y^2 and $\overline{\sigma_y^2}$, σ_z^2 and $\overline{\sigma_z^2}$.
s_0	Value of $s(\delta T)$ for $\delta T < 10$ minutes.
s_1	Free parameter in the frequency function $f_{\gamma_{1n}}$.
s_2	Free parameter in the frequency function $f_{\gamma_{2n}}$.
s_∞	Value of $s(\delta T)$ for $\delta T \geq 10$ minutes.
S	Number of scans required to produce one remote datum.
t	Time.
t_0	Initial time.
t_j	Instant in time at which the fast response <i>in situ</i> measurement applies.
t_{met}	Time scale during which the average values of the meteorological parameters apply.

LIST OF SYMBOLS (Cont.)

<u>SYMBOL</u>	<u>DESCRIPTION</u>
T	Time scale over which the direction of the mean wind, θ , coincides to a reasonable degree with the observed direction of the actual wind at any random instant in time in an interval of T duration.
T_0	Instrument lag time for remote measurement.
T_C	Instrument collection time for remote measurement.
T_R	Instrument response time for remote measurement.
T_y	Time constant for u_{1_y} , u_{2_y} , u_{3_y} , and u_{4_y} .
T_z	Time constant for u_{1_z} , u_{2_z} , u_{3_z} , and u_{4_z} .
T_η	T_y and/or T_z , as the case may be.
$u_{1_y}(t)$	Component of $\gamma_{1_y}(t)$.
$u_{2_y}(t)$	Component of $\gamma_{1_y}(t)$.
$u_{1_z}(t)$	Component of $\gamma_{1_z}(t)$.
$u_{2_z}(t)$	Component of $\gamma_{1_z}(t)$.
$u_{3_y}(t)$	Component of $\gamma_{2_y}(t)$.
$u_{4_y}(t)$	Component of $\gamma_{2_y}(t)$.
$u_{3_z}(t)$	Component of $\gamma_{2_z}(t)$.
$u_{4_z}(t)$	Component of $\gamma_{2_z}(t)$.
$u_{1_\eta}(t)$	$u_{1_y}(t)$ and/or $u_{1_z}(t)$, as the case may be.

LIST OF SYMBOLS (Cont.)

<u>SYMBOL</u>	<u>DESCRIPTION</u>
$u_{2_n}(t)$	$u_{2_y}(t)$ and/or $u_{2_z}(t)$, as the case may be.
$u_{3_n}(t)$	$u_{3_y}(t)$ and/or $u_{3_z}(t)$, as the case may be.
$u_{4_n}(t)$	$u_{4_y}(t)$ and/or $u_{4_z}(t)$, as the case may be.
\bar{U}	Mean wind speed, $\bar{U} \equiv \bar{\vec{V}} $.
v_{1_y}	Uncorrelated Gaussian process driving u_{1_y} equation.
v_{1_z}	Uncorrelated Gaussian process driving u_{1_z} equation.
v_{2_y}	Uncorrelated Gaussian process driving u_{2_y} equation.
v_{2_z}	Uncorrelated Gaussian process driving u_{2_z} equation.
v_{3_y}	Uncorrelated Gaussian process driving u_{3_y} equation.
v_{3_z}	Uncorrelated Gaussian process driving u_{3_z} equation.
v_{4_y}	Uncorrelated Gaussian process driving u_{4_y} equation.
v_{4_z}	Uncorrelated Gaussian process driving u_{4_z} equation.
v_{1_n}	v_{1_y} and/or v_{1_z} , as the case may be.
v_{2_n}	v_{2_y} and/or v_{2_z} , as the case may be.
v_{3_n}	v_{3_y} and/or v_{3_z} , as the case may be.
v_{4_n}	v_{4_y} and/or v_{4_z} , as the case may be.
v_g	The ground track speed of the remote platform.
v_z^2	Second moment of the uniform vertical distribution.

LIST OF SYMBOLS (Cont.)

<u>SYMBOL</u>	<u>DESCRIPTION</u>
$V\{\cdot\}$	Variance operator.
$\vec{V}(t)$	Instantaneous wind velocity.
$\overline{\vec{V}}$	Mean wind velocity.
V_C	Volume of the conical field of view in the remote measurement model.
$V_u(z)$	Uniform vertical distribution.
$V_1(x,z;H)$	Vertical concentration distribution of the steady-state (time averaged) plume.
x	In cartesian coordinate system (x,y,z) specific to a given source with an effective stack height H . x is the downwind distance along the mean wind direction, y is the crosswind distance and z is the vertical distance above the surface. The source is located at $(0,0,H)$ in this system.
x'	In cartesian coordinate system (x', y', z') , relevant to multi-plume formulation, oriented so that the origin is at a fixed position on the surface, x' and y' are arbitrary (although x' is usually made to point eastward), z' is the vertical direction above the surface. In this sytem, a given point source is located at (x'_0, y'_0, H) .
x_L	Downwind distance at which the effect of the mixing layer first becomes significant.
x_u	Downwind distance at which the vertical pollutant concentration distribution is approximately uniform, under the influence of a mixing layer.

LIST OF SYMBOLS (Cont.)

<u>SYMBOL</u>	<u>DESCRIPTION</u>
x_p	Hypothetical distance at which the power law relation for D_y^2 yields a value of $D_{y^\infty}^2$.
\bar{x}	$\frac{1}{2}(x_u + x_L)$.
x'_p	Hypothetical distance at which the power law relation for D_z^2 yields a value of $D_{z^\infty}^2$.
X or $X(x,y,z,t;H)$	The instantaneous pollutant concentration (material distribution) for the fluctuating plume.
\bar{X} or $\bar{X}(x,y,z;H)$	Pollutant concentration based on the steady-state (time averaged) Gaussian plume model employing variances σ_y^2 and σ_z^2 determined using optimum (minimum) averaging times δt , to average out plume fluctuations.
$\overline{\overline{X}}$ or $\overline{\overline{X}}(x,y,z;H)$	Pollutant concentration based on the steady-state (time-averaged) Gaussian plume model employing variances $\overline{\sigma_y^2}$ and $\overline{\sigma_z^2}$ determined using averaging times $\delta T > \delta t$ to average out plume fluctuations.
y	In cartesian coordinate system (x,y,z); see x description.
y'	In cartesian coordinate system (x', y', z'); see x' description.
y'_0	y' position of a given point source.
$\overline{y^2}$	Total average dispersion of the plume in cross-wind direction.
$\overline{Y^2}$ or $\overline{Y^2}(x)$	The variance (square of the width parameter) in the crosswind direction of the material distribution of the instantaneous fluctuating plume, relative to the instantaneous plume centerline.

LIST OF SYMBOLS (Cont.)

<u>SYMBOL</u>	<u>DESCRIPTION</u>
z	In cartesian coordinate system (x , y , z); see x description.
z'	In cartesian coordinate system (x', y', z'); see x description.
z'_0	z' position of a given point source.
$\overline{z^2}$	Total average dispersion of the plume in the vertical direction.
$\overline{z^2}$ or $\overline{z^2}(x)$	The variance (square of the thickness parameter) in the vertical direction of the material distribution of the instantaneous fluctuating plume relative to the instantaneous plume centerline.
$\gamma_{1_y}(t)$	Random process amplitude factor of $D_y(x,t)$.
$\gamma_{1_z}(t)$	Random process amplitude factor of $D_z(x,t)$.
$\gamma_{2_y}(t)$	Random process in the wavelength of $D_y(x,t)$.
$\gamma_{2_z}(t)$	Random process in the wavelength of $D_z(x,t)$.
$\gamma_{1_\eta}(t)$	$\gamma_{1_y}(t)$ and/or $\gamma_{1_z}(t)$, as the case may be.
$\gamma_{2_\eta}(t)$	$\gamma_{2_y}(t)$ and/or $\gamma_{2_z}(t)$, as the case may be.
δ	Exponent in power law for σ_y , $\delta \equiv p - 0.85$.
$\delta(\tau)$	The Dirac delta function.
Δ	Effective wavelength in $D_\eta(x,t)$ model development.
δt or $\delta t(x)$	Optimum time interval required to first average out meandering plume effects, i.e. the time interval required to view approximately the same value of the plume concentration more

LIST OF SYMBOLS (Cont.)

<u>SYMBOL</u>	<u>DESCRIPTION</u>
	than once. This amounts to the time required to advect the governing range of eddies past the observation point.
δT	Source instrument or measurement averaging time greater than δt .
δT_1	Lower limit in the transition range of δT for which the exponent $s(\delta T)$ significantly departs from s_0 .
δT_2	Upper limit in the transition range of δT for which the exponent $s(\delta T)$ is approximately equal to s_∞ (to the 95% level).
$\bar{\delta T}$	Midpoint in the transition range of δT in the $s(\delta T)$ relation, i.e. $\bar{\delta T} = \frac{1}{2}(\delta T_1 + \delta T_2)$.
$\delta T'$	A specific instrument averaging time.
$\delta \tau$	Characteristic time scales of the eddies governing the cross-wind fluctuations of the plume at some position downwind from the source.
$\Delta \tau$	Advective time scale associated with wind velocity \bar{U} and some space scale L , i.e. $\Delta \tau = L/\bar{U}$.
ΔH	The plume rise.
ϵ	Small positive number approximately equal to the inner stack diameter in $D_\eta(x, t)$.
ϵ_0	Random measurement errors of zero mean and variance σ_{obs}^2 in the remote measurement model.

LIST OF SYMBOLS (Cont.)

<u>SYMBOL</u>	<u>DESCRIPTION</u>
$\overline{\epsilon}_i$	Random measurement errors of zero mean and variance $\overline{\sigma_i^2}$ for time-averaged <i>in situ</i> measurement model. Subscript i refers to instrument at position \vec{r}_i .
ϵ_i^0	Random measurement errors of zero mean and variance $(\sigma_i^0)^2$ for instantaneous <i>in situ</i> measurement model. Subscript i refers to instrument at position \vec{r}_i .
ζ	In the cartesian coordinate system (ξ, η, ζ) and the cylindrical coordinate system (ρ, ψ, ζ) ; see ξ and ρ descriptions.
ζ_p	Altitude of the remote measurement platform.
η	In the cartesian coordinate system (ξ, η, ζ) ; see ξ description. Also used to indicate x and/or y in the (x, y, z) system. The appropriate description is evident from the specific context of the application.
θ	Azimuthal angle of the mean wind \bar{U} measured counter-clockwise from the x' -axis or eastward direction.
λ	Exponential dependence in $q(x)$ expression.
Λ	Exponential dependence in $Q(x)$ expression.
μ_{i_η}	Inverse of the time constant in the u_{i_η} equations, i.e. $\mu_{i_\eta} = \frac{1}{T_\eta}, \quad i = 1, 2, 3, 4.$
ξ	In the cartesian coordinate system (ξ, η, ζ) , ξ is the downwind direction, η is the crosswind direction and ζ is the altitude above the surface. The origin is at the position of the centroid of the remote measurement footprint (x_0, y_0) on the surface of the earth.

LIST OF SYMBOLS (Cont.)

<u>SYMBOL</u>	<u>DESCRIPTION</u>
π	The value of 3.1459...
ρ	In the cylindrical coordinate system (ρ, ψ, ζ) , ρ is the radial coordinate ($\rho^2 = \xi^2 + \eta^2$), ψ is the angle measured from the downwind direction (ξ -axis) and ρ, ζ is the altitude above the surface. The origin is at the position of the centroid of the remote measurement footprint (x_0, y_0) on the surface of the earth.
ρ_0	Radius of the circular remote measurement footprint.
σ_y or $\sigma_y(x)$	Standard deviation of width parameter of the steady-state Gaussian point source plume concentration in the crosswind direction. Unless noted otherwise, $\sigma_y(x)$ is based on the optimum time average that just averages out the fluctuations of the instantaneous plume at position x .
σ_z or $\sigma_z(x)$	Standard deviation or thickness parameter of the steady-state Gaussian point source plume concentration in the vertical direction. Unless noted otherwise, $\sigma_z(x)$ is based on the optimum time average that just averages out the fluctuations of the instantaneous plume at position x .
σ_y^0	Coefficient in the power law of $\sigma_y(x)$.
σ_z^0	Coefficient in the power law for $\sigma_z(x)$.
σ_z^1	Constant in certain formulations of the $\sigma_z(x)$ dependence.
σ_y^2	Variance or square of σ_y .
σ_z^2	Variance or square of σ_z .

LIST OF SYMBOLS (Cont.)

<u>SYMBOL</u>	<u>DESCRIPTION</u>
$\overline{\sigma_y}$ or $\overline{\sigma_y}(x, \delta T)$	Standard deviation (width parameter) of the time-averaged plume concentration (steady-state Gaussian plume) in the crosswind direction relevant to observations at downwind distance x with averaging time δT .
$\overline{\sigma_z}$ or $\overline{\sigma_z}(x, T)$	Standard deviation (thickness parameter) of the time averaged plume concentration (steady-state Gaussian plume) in the vertical direction relevant to observations at downwind distance x with averaging time δT .
$\overline{\sigma_y}^2$	Variance or square of $\overline{\sigma_y}$.
$\overline{\sigma_z}^2$	Variance or square of $\overline{\sigma_z}$.
$\overline{\sigma_z}^*$	Power law expression for $\sigma_z(x, \delta T)$ in the absence of mixing ceiling influences.
σ_V^2	Second moment of the vertical concentration distribution V_1 .
σ_V^*	Functional component of the $\sigma_z(x)$ expression when effects of the mixing layer are significant.
$\sigma_u(L, H)$	Limiting value of the thickness parameter $\sigma_z(x)$ to fit V_1 to V_u .
σ_u or $\sigma_u(L, 0)$	Value of $\sigma_u(L, H)$ for the case when $L \gg H$.
$\sigma_\theta(\delta T)$	Crosswind standard deviation of the mean wind direction for averaging time δT .
σ_{obs}^2	Variance of the remote measurement noise.
$\overline{\sigma_i}^2$	Variance of the time averaged <i>in situ</i> measurement noise.

LIST OF SYMBOLS (Cont.)

<u>SYMBOL</u>	<u>DESCRIPTION</u>
$(\sigma_i^0)^2$	Variance of the instantaneous <i>in situ</i> measurement noise.
$\Sigma_n(x)$	In the model of $D_\eta(x,t)$, $\Sigma_n(x) \equiv \overline{D_\eta^2(x)}$.
$\sum_{i=1}^n$	Summation over all values of the index from 1 through n.
τ	Some time value.
ϕ	Elevation angle of the mean wind (taken to be zero in value) or the half-angle field of view of the remote measurement. The appropriate description can be determined from the context of the application.
$\overline{\phi}(t)$	The remote measurement at time t.
$\overline{\phi}_\zeta$	The integral over ζ in the $\overline{\phi}$ expression, $\overline{\phi}_\zeta \equiv \overline{\phi}_{\zeta+} + \overline{\phi}_{\zeta-}$.
$\overline{\phi}_{\zeta-}$	Portion of the integral over ζ in the $\overline{\phi}$ expression that corresponds to the original point source at $\zeta = H$.
$\overline{\phi}_{\zeta+}$	Portion of the integral over ζ in the $\overline{\phi}$ expression that corresponds to the fictitious average source at $\zeta = -H$.
$\overline{\phi}_{\zeta\infty}$	Approximation of $\overline{\phi}_\zeta$ obtained by replacing the conical volume V_C by an infinite vertical cylinder.
$\overline{\phi}_\infty(t)$	Approximation of $\overline{\phi}(t)$ obtained by replacing the conical volume V_C by an infinite vertical cylinder.
$\overline{\phi}_{\eta\infty}$	The integral with respect to η in the $\overline{\phi}_\infty(t)$ expression.
ψ	In the cylindrical coordinate system (ρ, ψ, ζ) ; see description of ρ .

LIST OF SYMBOLS (Cont.)

<u>SYMBOL</u>	<u>DESCRIPTION</u>
$\Psi_{ij}(\vec{r}_i, t_j)$	Instantaneous <i>in situ</i> point measurement for instrument at position \vec{r}_i and time t_j .
$\bar{\Psi}_i(\vec{r}_i)$	Time averaged <i>in situ</i> point measurement for instrument at position \vec{r}_i .
$(\bar{\Psi}_i)_{t_j}$	Time averaged <i>in situ</i> point measurement for instrument at position \vec{r}_i , taken over a time interval beginning at t_j .
$\omega_\eta(x)$	In the model for $D_\eta(x, t)$, $\omega_\eta(x) = 2\pi/[\epsilon(\epsilon + f_\eta(x))]$.
$\frac{d}{dt}[\cdot]$ or $[\cdot]$	Derivative with respect to time of the variable in brackets.
\rightarrow	Goes to or approaches.
\sim	On the order of.
\equiv	Identically equals or is defined as.
$<$	Less than.
$<<$	Much less than.
\leq	Less than or equal to.
\lesssim	Less than or approximates.
\approx	Approximately equal to.
$>$	Greater than.
$>>$	Much greater than.
\geq	Greater than or equal to.

LIST OF SYMBOLS (Cont.)

<u>SYMBOL</u>	<u>DESCRIPTION</u>
\geq	Greater than or approximates.
∞	Infinity.
\oint_{V_C}	Integral over the volume of V_C .
\oint_{A_0}	Integral over the area of A_0 .
$\langle \cdot \rangle_{\delta T}$	Rigorously computed mathematical average over the time interval δT of the quantity in brackets.

I. INTRODUCTION

National concern about the impact of environmental pollution on the quality of life has provided increasing motivation for efforts to obtain precise information about existing air quality, particularly for large urban areas. Traditionally, this information has been obtained using *in situ* sampling methods. Unfortunately, the area-wide high accuracy concentration determinations now desired would impose prohibitive cost burdens in the form of a closely spaced network of fixed ground-based sampling stations using these traditional measuring techniques. The attempts at deriving air quality information through the use of pollutant diffusion simulation computer models are also severely restricted due to the limitations of the basic assumptions and gross uncertainties in the fundamental physical parameters of the model and other necessary input information.

Remote measurement systems such as the instruments under development at the Langley Research Center designed for operation from aircraft or satellite platforms, offer the prospect of large amounts of data concerning urban air pollution levels. However, remote sensors provide spatially integrated instantaneous measurements, which because of their frequently poor vertical resolution, will have to be supplemented by the generally sparse set of *in situ* ground based measurements that represent spatially localized and often time-averaged values. It appears that in order to provide area-wide air quality information to an adequate level of accuracy, a variety of measurement types will have to be combined in some way with diffusion model simulations. The combination of measurements with air pollution simulation models introduces further difficulties in that operational models for the most part employ steady-state assumptions that only provide a valid representation of the spatial distribution of pollutants in some time-averaged sense.

Urban air quality estimation involves the concepts of "*urban air quality and estimation*". "*Urban air quality*" is a familiar concept: it involves specification of the concentration of various pollutants as a function of position over the urban area. In addition, these concentrations are referred to particular representative meteorological conditions and particular averaging times, e.g. daily or monthly averages or possibly even a particular instant in time. "*Estimation*", as employed here, is a rather specific engineering concept which is perhaps less familiar, so a definition is in order:

"Estimation is a methodology for utilizing information contained in measurements to improve ones knowledge of the relevant physical processes in this case, pollution dispersion."

The major objective of the current contract is to study the possibilities for the application of estimation theory to the analysis, interpretation and use of urban air quality measurements in conjunction with simulation models to provide a cost-effective method of obtaining reliable air quality estimates for wide urban areas. The goal is a methodology for utilizing *all the available data* in a *self-consistent* manner in conjunction with *air pollutant dispersion models* and *a priori information*. An *estimator* (or estimation algorithm) incorporates a measurement into a model *update*, i.e. an update of the *states* or parameters describing the pollution dispersion process. To do this, one requires not only a parameterized model which describes the physical processes (i.e. *a pollutant dispersion model*) but *measurement models* consistent with the measurement devices and measurement processes of interest, as well. These two levels of modeling involved in the estimation process must be mutually consistent in terms of their fundamental assumptions and approximations. The same internal consistency is required for the incorporation of any *a priori* information concerning the physical processes and model parameters. Estimation theory, which originated in guidance and control research, can ultimately lead to the development of software for the sequential update of diffusion model estimates of pollutant distributions with measured air quality data on a real-time basis.

Before the development of an actual estimator could be initiated, the requirement for mutual consistency between the various levels of modeling, the measurements and *a priori* information necessitated undertaking a basic research and development effort. This effort has sought to bridge an existing gap in the state-of-the-art in relating air quality measurements taken on different time scales (particularly, fast response measurements applicable to a short time scale) with standard air pollutant dispersion models which are only valid representations in some time-averaged sense.

The typical urban air quality control region represents a wide variety of pollutant source conditions ranging from relatively isolated, but frequently large point sources such as a group of power plant stacks located in the suburbs, major line sources representing the principal highways, many lesser low level

sources in close proximity typical of area source representations, to the conglomeration of all source categories that represents the high density conditions of the inner city. The major emphasis during the first phase of the contract has been on the elevated point source. This category represents the principal source type for many pollutants and is characterized by a particularly complex phenomenology presenting serious difficulties for relating measurements and dispersion models.

Measurement models development has emphasized the categories:

- (1) Fast response spatially integrated (long path or volume) values typical of remote based measurements from aircraft or satellite platforms.
- (2) Fast response and time-averaged point values typical of *in situ* measurements from ground based fixed site or mobile platforms.

While these measurement types are the immediate concern of the present contract, the theoretical modeling effort is not inherently restricted to these types. Measurement models for other systems, such as ground based remote measuring devices, can be immediately incorporated into the total modeling framework, once their specialized mathematical representations have been formulated.

There are a number of alternate mathematical techniques that can be applied to the solution of the combined simulation modeling and estimation problem using measurement data. These techniques essentially parallel the approaches that can be applied to the solution of the pollutant diffusion problem, in isolation, without the incorporation of air quality measurements. One can formulate the diffusion problem as a partial differential equation with initial conditions and boundary values and proceed with a direct numerical solution of the resulting system. Standard solution techniques include finite differences and eigenfunction expansions or a variety of other complete function representations. Recently, A. A. Desalu (1974) applied finite difference techniques to the simulation and air quality estimation problem and K. D. Pimental (1975) applied an eigenfunction expansion approach in a similar context. Another technique is to employ quasi-empirical "special" solutions based on actual solutions to special cases of the (simplified) partial differential equation representation and experimental observations. An example of this approach, to the air quality estimation problem, using the Gaussian point source steady state plume representation is given by Smith, Green and Young (1974a,b). The "special" solution approach is the one that has been adopted here

for the current research effort with attention given to both time-averaged and instantaneous plume representations.

The techniques based on direct solution of the partial differential equation (i.e. finite difference and functional expansions) have the advantage of being structurally and formally simpler, having been explored and analyzed in a more or less independent mathematical context. However, the practical application of the method to an urban scale area results in a computationally enormous problem because the wide distribution of primary pollution sources requires the use of a fairly fine grid over the entire region. For example, using a one kilometer grid to simulate the diffusion process below the tropopause over a 100 km x 100 km urban area yields a total of about 10^5 concentration points which must be solved for in the simulation and estimation problem. In terms of estimation techniques, this is beyond the current state-of-the-art. Similarly, the large area and multi-source environment requires a large number of eigenfunctions to properly represent the concentration distribution to any reasonable degree of accuracy. The partial differential equation approach also has difficulty representing the effects of atmospheric turbulence and the stochastic fluctuating plume on any short time scale. The subgrid (spatial) scale phenomenon (or equivalently the short wavelength phenomena beyond the representation of the truncated eigenfunction expansion) require a deterministic approximation of the statistics, in any event. As a result of these difficulties, application of these techniques has not progressed to any large scale practical applications.

The special solution methods have the disadvantage of requiring sophisticated techniques to treat the spatial variation of concentration. However, the input/output is conceptualized better through a more direct relation to the current diffusion models. The model parameters are conveniently expressed in terms of *a priori* experimental observations, since these experimental observations have generally been taken into account in the original model formulation. Propagation in time is generally simple and the representation of time averaged measurements is also simple. Stochastic plume properties, while still complex, can also be modeled. The model parameters, in being directly related to the observed physical processes, offer a generally simplified analysis of sensitivity to physical parameters. The computational complexity of the full scale urban simulation and estimation problem is directly proportional to the number of sources present (rather than the overall area). However, the required computational power is

usually much less than would be required by direct solution of the partial differential equation techniques.

A general discussion of the physical phenomenology of real atmospheric plumes from elevated localized sources is given in Section II. That section provides background for the actual plume dispersion model development discussed in Section III. The derivation of a fluctuating plume model presented in Section III, follows the development given by Gifford (1959), but adds a reflection condition at the lower boundary to provide a model that is mathematically related (through the expected value) to the time-averaged plume model of Turner (1970). In Section IV, the individual plume parameter formulations are developed along with the associated *a priori* information. Section V provides the last major modeling link required to apply estimation theory, the development of individual measurement models. The measurement models presented in Section V emphasize general forms applicable to: (1) remote measurement systems based on aircraft and satellites, (2) *in situ* measurement systems.

**Page
Intentionally
Left Blank**

II. PROPERTIES OF REAL PLUMES FROM ELEVATED POINT SOURCES RELATED TO THE PROBLEMS OF DISPERSION AND MEASUREMENT MODELING

The continuous emissions from a small elevated isolated source of emissions, such as a smoke stack, is the basis of the mathematical idealization of the *point source*. The emissions from such a source usually take on the form of a plume. These plumes probably are the subject of the vast majority of all experimental and theoretical work in the field of air pollution meteorology and the mathematical models that have been developed to represent them are integral components of most of the operational urban air pollution simulation models. Furthermore, since tall stacks from industrial facilities and power plants are representative point sources in many cases they are the most important components of the urban air pollution scenario. Consequently, point source plumes provide a logical place to begin consideration of the problems of relating disparate measurement types and air pollution models.

While the concept of a continuous emitting point source may appear simple, in reality it encompasses in microcosm most of the difficulties encountered in air pollution measurement, estimation and modeling. Even at this time, a great deal is still not known about the details of the physics of plume dispersion in the real atmosphere.

The phenomenon of plume formation is a consequence of:

- (a) Advective transport by the coherent motions of the atmosphere (winds).
- (b) Dispersive transport by the random fluctuations due to atmospheric turbulent eddies.
- (c) Dispersive transport by molecular scale diffusion processes.

The molecular and turbulent diffusion processes both produce a similar average transport of pollutants in a direction opposite to the local concentration gradient. However, the effects of turbulence predominate to such a degree that the molecular effects can be ignored in comparison. Similarly, under normal atmospheric wind conditions, the turbulent eddy diffusion in the direction of the local wind can usually be neglected in comparison with the advective transport. However, for the real transient processes in the atmosphere, the demarcation between incoherent

turbulence and the coherent winds which produce advection is somewhat arbitrary. While the local transient winds will have a component due to the repeatable discrete weather patterns, another time-varying component will in fact be produced by the largest scale eddies. In terms of plume dispersion the demarcation line is between eddies much larger in dimension than the *instantaneous* plume width and all eddies below the scale of the instantaneous plume width.

The very large eddies contribute to changes in the instantaneous wind vector, \vec{V} . The very smallest eddies cause slight dispersive spreading of the plume, but eddies about the same size as the local plume width are the most effective in producing turbulent plume dispersion. Eddies larger than the instantaneous plume width but smaller than the characteristic horizontal scale of the region of interest (typically, the downwind distance from the source) produce the meandering character of the real instantaneous plume. In summary, if ℓ is the characteristic eddy dimension, L is the characteristic horizontal scale of the region, D is the average instantaneous plume width, then the role of eddies in plume dispersion is given by:

- (1) $\ell \ll D$, slight plume dispersion and internal plume mixing.
- (2) $\ell \sim D$, most effective in plume dispersion.
- (3) $D < \ell \leq L$, produces plume meandering.
- (4) $\ell > L$, produces changes in the wind vector.

The physics of plume dispersion has certain inherent time scales which are related to the space scales associated with the different eddy ranges discussed above. These time scales, in turn, describe different phenomenological aspects when associated with the concepts of "averaging times" or "sampling times" which one is inevitably led to in describing or measuring any phenomenon having an important stochastic element. These different phenomenologies, associated with the different time and space scales, produce the major difficulty in relating a particular measurement type to any idealized description or mathematical model which only addresses a particular phenomenological aspect.

One time scale of interest is the value of T which will allow the direction of the mean wind, \vec{V} , to coincide to a reasonable degree with any observation of $\vec{V}(t)$ (i.e. small variance): Experience suggests a value of no more than 2-3 hours (Slade, 1968). For observations extending over times much longer than this, the wind is likely to take on the full range of directions. The isopleths of pollution concentration,

correspondingly time-averaged, will form an approximately concentric pattern about the source with evident off-sets in the pattern, corresponding to any preferential directions of the wind. The pattern generally will not resemble a plume.

If a plume is photographed or measured by any device having an averaging time on the order of a fraction of a second, the appearance will have a sinuous form. The sinuosities appear to increase in amplitude and characteristic wavelength as one observes at greater distances from the source. The increase in amplitude as a function of source distance is a subject of frequent discussion in the literature on turbulent plume diffusion (e.g. Scorer, 1968), while the apparent increase in characteristic wavelength with distance is not. Nevertheless, it seems to be a quite observable feature in published photographs of many real plumes in the atmosphere (Scorer, 1968 and Slade, 1968) as well as in photographs of plumes generated in wind tunnels (Williamson, 1973). The mechanisms invoked to explain the amplitude increase of the instantaneous plume would seem to suffice to explain the increase in characteristic wavelength also.

Generally, eddies of all scales can be expected to be present in the atmosphere but not necessarily to an equal degree. Near the source, the diffusive spreading of the plume is produced by the small turbulent eddies comparable in scale to the initial plume width. As the plume is advected downwind, the instantaneous plume spreads horizontally and vertically and also tends to meander within more or less definite limits. The amplitude of the crosswind and vertical meandering increases as the plume is advected downwind, as does the apparent effective wavelength of the sinuosities. The increasing crosswind and vertical spreading in the downwind direction constantly brings into play larger scale eddies which become the most effective in spreading the instantaneous plume: the next larger class of eddies which produce the meandering quality, consequently also increases in scale in the downwind direction. If all scales of eddies are present in the atmosphere to an equal degree, the fact that distance from the source origin is the only dimension of consequence would require the envelope of the meandering plume to take the form of a cone based on arguments of similarity. In the atmosphere there are many real conditions which cause eddies of certain scales to be present to a greater or lesser degree than eddies of other scales, so that the angle of the cone may change some distance downstream. Based on the above observations, one would expect the effective wavelength of the sinuosities to increase in the downstream direction, since this "effective" wavelength must also be characteristic of the dominant

scale of the eddies producing the meandering effect.

The description of the plume physics given above intimately associates the spatial scale of eddies governing the phenomena of plume spread and meander with the downwind distance from the source. However, the description also implies certain time scales which together with these space scales dictate the state of the plume actually measured or observed. In the first place, the downwind distance from the source origin, L , can be associated with a time, $\Delta\tau$, based on the fact that transport in that direction is mostly due to advection. Therefore, the mean wind speed, $\bar{U} \equiv |\bar{\vec{V}}|$, is the connecting parameter:

$$L \sim \bar{U} \Delta\tau$$

Similarly, at any given downwind distance L , there is some associated spatial range of eddies. Measurements or observations of the plume made at position L would have to be repeated over some time interval, δt , in order to view approximately the same values of the state more than once, i.e. in order to just average out the meandering effects. The time δt must be associated with the time interval required to advect the governing range of eddies past the observation point. Since the scale of eddies ℓ is not a single well defined value, the time scale of δt is also not well defined. However, in some sense, we would expect

$$\ell \sim \bar{U} \delta t$$

or

$$\delta t = [\ell / \bar{U}]_{\max}$$

Since ℓ is proportional to L and $|\vec{V}| \sim |\bar{\vec{V}}|$, clearly δt increases downstream from the source. In terms of meandering, we know that ℓ is bounded by L , so that if $\bar{U} \sim 5\text{m/sec}$ (~ 10 miles/hr.):

$$\left. \begin{array}{l} \delta t \sim 20 \text{ seconds, } L \sim 100 \text{ m} \\ \delta t \sim 3 \text{ minutes, } L \sim 1 \text{ km} \\ \delta t \sim 15 \text{ minutes, } L \sim 3 \text{ miles} \\ \delta t \sim 1/2 \text{ hours, } L \sim 10 \text{ km} \\ \delta t \sim 5 \text{ hours, } L \sim 100 \text{ km.} \end{array} \right\} .$$

These time scales seem to be borne out by experience (Scorer, 1968 and Slade, 1968).

We have previously described the qualitative picture of the instantaneous plume. Very little is known about the instantaneous material distribution cross-sectional to the plume. The form of the instantaneous distribution will be a function of the initial conditions and, again, the averaging time associated with the "instantaneous" observation. Close to the source, the influence of the initial conditions will be strongest, but since the processes of atmospheric motion are dissipative, one can expect these influences to diminish downstream from the source. Close to the source, the measurement time must also be fairly short in order to differentiate between the instantaneous plume and the plume averaged over the short period meandering motions. Consequently, observations of the instantaneous plume for small distances L can be expected to show a rather irregular cross-sectional material distribution. However, for large distances L , the irregularities due to initial conditions can be expected to be sharply reduced. Also, longer measurement times can be made of the instantaneous plume without averaging out the meandering motion. For long measurement times, the small scale turbulent eddies can be expected to smooth the material distribution in the "instantaneous" plume, so that its form may be similar to the cross-sectional distribution obtained by averaging over the meandering motions. A truly instantaneous view could be expected to portray an irregular cross-sectional material distribution at any distance L .

For the average plume, an assumption that each quantum of pollutant is undergoing a random walk type of process leads to the conclusion that the density function for each such quantum is Gaussian (at least asymptotically with downstream distance), regardless of the nature of the driving noise. (In fact the driving forces are the macroscopic eddies and the microscopic diffusion forces which, because of their wide bandwidth, are probably a good approximation to a Gaussian process.) Measurements of the average material distribution crosswind and vertical to the plume tend to appear Gaussian. Consequently, the average plume appears to have a more or less smooth boundary of conical form with the axis aligned with the mean wind direction. At any downwind position, L , the cross-sectional material distribution is a bivariate Gaussian function centered on the plume axis with principal axes in the vertical and horizontal directions. The boundary is in fact the envelope of various positions of the meandering plume. The conical appearance is dramatically revealed in time lapse photographs of real atmospheric plumes (Slade, 1968) and wind tunnel tests (Williamson, 1973).

Based on conservation of mass arguments, one would expect the time averaged Gaussian cross section for the cross-sectional material distribution of a constant strength localized source (idealized as a point) to become less sharply peaked (i.e. maximum concentration decreases) at further positions downwind. This is supported by observations. Any settling or other scavenging processes will tend to still further decrease the observed peak concentrations in the downwind direction in both the instantaneous and average plumes. By the same conservation of mass arguments, the mass distribution of any cross-section of the instantaneous plume must be more sharply peaked (i.e. greater maximum concentration) than the time averaged mass distribution at the same distance downstream, whatever the actual shape of the instantaneous mass distribution may be.

Expansion of the average plume, along an ideal constant angle cone up to some downwind distance L_0 will only be perceived if a continuous range of turbulent eddies up to and including a characteristic dimension L_0 are present in the atmosphere to an equal degree or intensity, and if measurements at each position L for $0 < L < L_0$ are averaged over a time interval, δT , such that:

$$\delta T = \delta t(L),$$

where $\delta t(L)$ is the characteristic time-scale of the dominant class of eddies responsible for the meandering motions at position L . If, as is frequently the case in real atmosphere (particularly under stable conditions) a whole range of eddies is almost entirely absent, the angle of the cone will be sharply reduced at some position L . On the other hand, if topographical features or other influences cause a particular class of eddies to have a greater intensity, the angle of the cone will expand at some position L where the class of eddies becomes dominant (Scorer, 1958).

The question now arises as to how the average plume will be manifested when viewed or measured with an instrument that has a *fixed* averaging time:

$$\delta T = \delta T' = \text{constant}.$$

Clearly, $\delta T'$ can correspond to the characteristic time scale of the dominant eddies that produce meandering near only one downstream position L' :

$$\delta T' = \delta t(L')$$

For all positions $0 \leq L \leq L'$, $\delta T'$ will be *longer* than the characteristic time scale $\delta t(L)$ of the eddies that produce meandering and for all positions $L' < L \leq L_0$, $\delta T'$ will be *shorter* than the characteristic time scale $\delta t(L)$.

When $L \gg L'$, then $\delta t \gg \delta T'$ and one can expect to view what is essentially the "instantaneous" meandering plume with a possibly non-Gaussian cross-sectional concentration distribution having a central peak offset from the axis of the mean wind. This is precisely the situation viewed in time lapse or superimposed photographs of plumes for distances far enough downwind (Williamson, 1973). There is likely to be some intermediate region $L \geq L'$ so that $\delta t \geq \delta T'$. In this case more than one realization of the instantaneous plume may be viewed, but not enough samplings will be taken to obtain the proper average (Gaussian) cross-sectional concentration distribution. In this case the average concentration distribution may exhibit more than one well defined peak on the scale of the instantaneous plume width. However, one would expect this intermediate downwind region to be represented by a very short interval in the x direction. There is also likely to be some intermediate region of the plume $L \leq L'$, where $\delta t \leq \delta T'$. In this case, the averaging time of the instrument will be just about right and the earlier discussion concerning the conical envelope of the average plume with a Gaussian cross-sectional concentration distribution aligned with the axis of the mean wind will hold. For $L \ll L'$, then $\delta t \ll \delta T'$ and the averaging time of the instrument will include the effects of eddies larger than the dominant class of eddies responsible for meandering: the motion of these eddies would normally be ascribed to the coherent wind by an observer fixed at that location. Here, the averaging includes some deviations from the mean wind with meandering motion superimposed on each coherent wind direction. This amounts to averaging a number of Gaussian cross-sectional concentration distributions having different central axes. Again the cross-sectional concentration distribution in the region $L \ll L'$ will be Gaussian. The envelope will again be a smooth curve of the conical form with the axis oriented in the direction of the mean wind. The envelope will be wider than the optimum conical form originally discussed and consequently the Gaussian concentration distribution will be broader and flatter at corresponding downstream positions.

The discussion of this section has been implicitly concerned with "pure plumes" in the atmosphere. Pure plumes are assumed to emerge from the source orifice with negligible exit velocity and essentially the same thermodynamic state as the ambient atmosphere. In that case the plume dispersion is due entirely to the coherent wind and ambient atmospheric eddies. In reality, the source emissions have momentum due to a non-negligible exit velocity, different density due to the effluent composition, different temperature (usually higher) due to the energy conversion and industrial chemical processes usually associated with sources, and definite vorticity mainly due to mechanical design factors. A plume which is principally distinguished by initial momentum differences is often referred to as a "jet". A plume distinguished by initial bouyancy is often referred to as a "bouyant plume" and exhibits an initial "plume rise". Initial momentum will also contribute to plume rise.

III. INSTANTANEOUS AND TIME AVERAGED POINT SOURCE PLUME MODELS

Many operational air pollution simulation models (Koch and Fisher, 1973) have the Pasquill-Turner point source formulation (Turner, 1970) as a basic component. It is also the model employed by Smith, Green and Young (1974a,b) for interpretation of pollution measurements from aircraft and satellites. This relation is given by:

$$\frac{\bar{X}(x,y,z;H)}{Q} = \frac{1}{2\pi\sigma_y\sigma_z\bar{U}} \exp\left[-\frac{1}{2}\left(\frac{y}{\sigma_y}\right)^2\right] \times \left\{ \exp\left[-\frac{1}{2}\left(\frac{z-H}{\sigma_z}\right)^2\right] + \exp\left[-\frac{1}{2}\left(\frac{z+H}{\sigma_z}\right)^2\right] \right\}, \quad (1)$$

where \bar{X} is the pollution concentration, Q is the source strength (average pollutant mass production rate), \bar{U} is the mean wind speed, H is the effective height of the point source, σ_y is the standard deviation, or more properly the *width parameter*, of the plume concentration in the cross-wind direction and σ_z is the standard deviation or *thickness parameter* of the plume concentration in the vertical direction. The Cartesian coordinate system (x,y,z) is oriented so that z is the vertical distance above the surface of the Earth, x is the distance (down-wind) along the mean wind direction and y is the cross-wind distance. In this coordinate system, the point source is at the position $(0,0,H)$.

The (x,y,z) coordinate system described above is not convenient if more than one source is to be considered. Let (x',y',z') be a Cartesian coordinate system such that the z' axis is again in the vertical direction, the origin is at some point on the surface of the Earth and the x' and y' axes are otherwise arbitrary. Let the source be at position (x'_0, y'_0, H) in this coordinate system. Then the two coordinate systems are related through the transformations:

$$\left. \begin{aligned} x &= (x' - x'_0) \cos \theta + (y' - y'_0) \sin \theta \\ y &= -(x' - x'_0) \sin \theta + (y' - y'_0) \cos \theta \\ z &= z' \end{aligned} \right\} \quad (2)$$

where θ is the azimuthal angle of the mean wind \bar{U} measured counter-clockwise from the x' -axis. The elevation angle ϕ of the mean wind is equal to zero.

Equation (1) is based on the assumption of a steady state point source. Consequently, the expression can only be related to real atmospheric plumes in a time-averaged sense. The dispersion of pollutants in a real plume, when considered at any *instant in time*, consists of two parts:

- (a) The gradual vertical and crosswind spreading of the plume proper, as the bulk of the emissions is advected downwind,
- (b) The sinuous motions which cause the bulk of the plume to constantly fluctuate in the vertical and crosswind directions as the emissions are advected downwind.

Only when the plume is viewed over some *finite time* interval, do the sinuous motions average out to produce the regular appearance of the time averaged or steady-state plume depicted by the dashed-line envelope of Figure 1a. The fluctuating aspect of the plume when viewed at an instant has given rise to the notion of a "fluctuating" plume. This phenomenon, illustrated schematically in Figure 1a, can be explained in terms of the effects of eddies of different physical scales. These concepts have been discussed previously in Section II.

The subject of fluctuating plumes has provided a relatively scant amount of published materials of either a theoretical or experimental nature compared to the subject of steady state or time averaged plumes. Much of the material that is available is in the form of Ph.D. dissertations and other limited distribution technical reports. While a degree of mathematical modeling has been done, this has generally not been extended to applications in air pollution computer simulation models to date. An area of theoretical work that has found its way into the more generally available formal literature is the fluctuating plume model due to Frank Gifford, Jr. (Gifford, 1959). The model developed by Dr. Gifford has the desirable property of being related to time averaged plume models through formal statistics. Consequently, this is a logical place to begin the estimation problem (i.e., relating more or less instantaneous measurements of real plumes to steady state plume models).

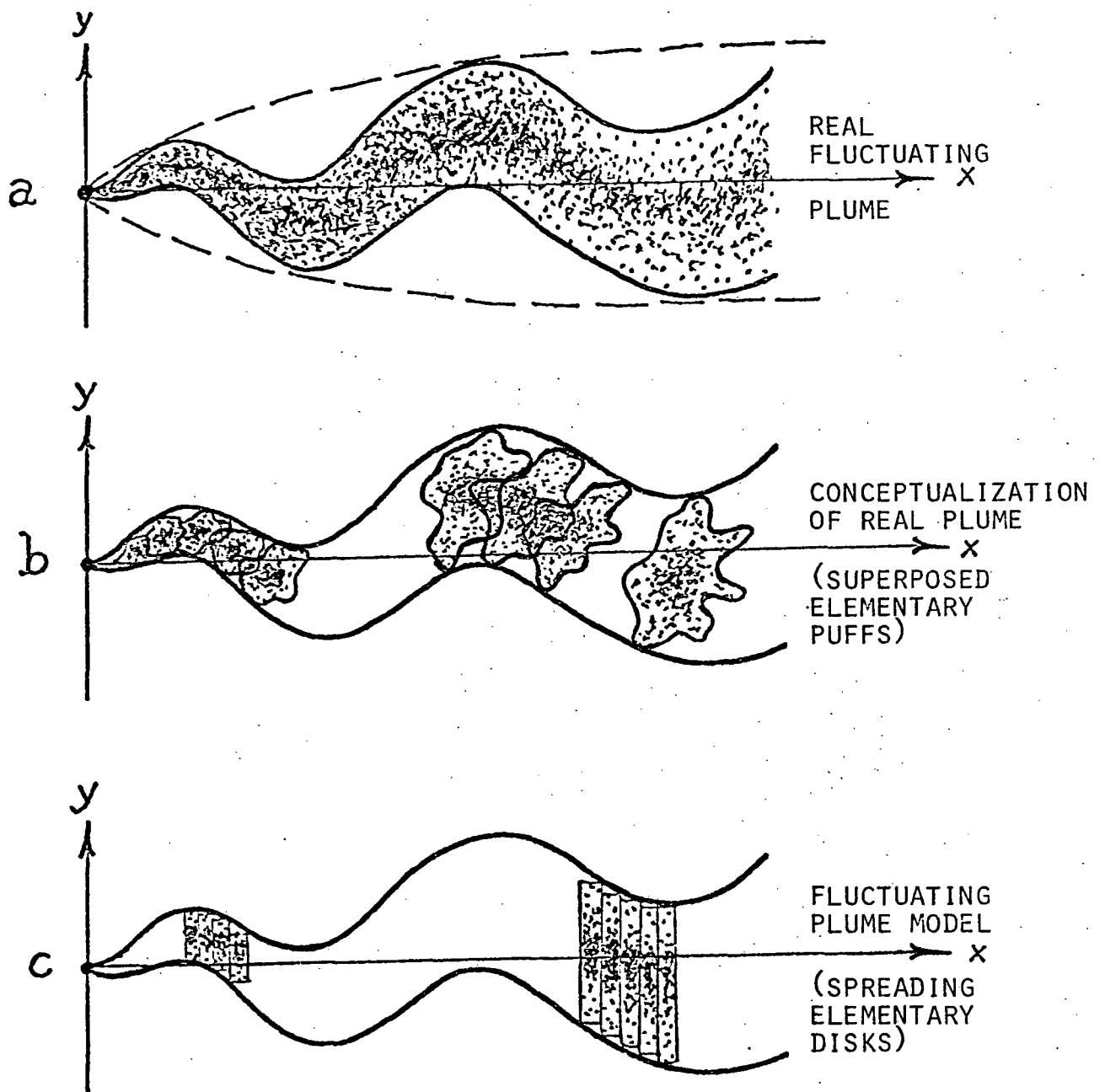


Figure 1. Various Schematic Representations of A Real Instantaneous Plume Leading to Mathematical Modeling

Conceptually, the real plume may be thought of as consisting of an infinite series of over-lapping emission *puffs*, each released some infinitesimal time interval second after the preceeding one. Each puff, as it is transported with the mean wind, meanders and expands diffusively in the crosswind, vertical and downwind (x-axis) directions. This concept is illustrated schematically in Figure 1b. If we neglect the diffusive transport in the downwind direction compared to the advective transport, then each puff need only be thought of as diffusively spreading in the vertical and crosswind directions as it meanders downwind. This leads to the "spreading elementary disk model" of the instantaneous plume proposed by F. Gifford (1959) and illustrated schematically in Figure 1c.

The x-axis, aligned with direction of the meanwind, is assumed to represent the centerline for the average plume. At any instant, the center of a particular disk is conceived of as having a *random* displacement (D_y, D_z) from the fixed position of the x-axis. The material distribution, X of any particular disk is given by:

$$\frac{X}{Q_d} = f(y-D_y, z-D_z, t; y_0, z_0, t_0, \bar{U}) \quad (3)$$

where Q_d is the total amount of material in the disk, t is the time, y is the crosswind direction, z is the vertical direction, \bar{U} is the mean wind speed (in direction of x-axis), the subscript "zero" refers to initial conditions, and f is the material distribution function *centered at the position* (D_y, D_z) from the origin.

Much of Gifford's basic derivation follows by induction from the special case of dispersion of a one-dimensional cloud (Gifford, 1959):

$$\frac{X}{Q_d} = f(y-D_y, t; y_0, t_0) \quad (4)$$

If a coordinate system is fixed with respect to the mean wind \bar{U} and observations are made of a single realization of a cloud (or disk) for successive values of t , D_y will vary irregularly due to the turbulent eddies. This variation of D_y is assumed to be random. On the other hand, a number of realizations of the elementary clouds may be viewed for successive values of t_0 . If observations are made of this ensemble for fixed values of dispersion time, $t-t_0$, then these observations of D_y will also be seen to fluctuate statistically. If an ensemble average is taken over many trials:

$$E \left\{ \frac{X}{Q_d} \right\} = \int_{-\infty}^{\infty} f(y-D_y, t; y_0, t_0) g(D_y) dD_y \quad (5)$$

Here, $g(D_y)$ is the frequency function for the variability of D_y over the different realizations. E indicates the *expected value* or *mean* operator.

Equation (5) assumes that the form of f is either fixed or completely correlated with D_y . Actually the form of the function f varies from trial to trial because of the influence of initial conditions and a limited sampling of turbulent fluctuations in the dispersion time $t-t_0$. The basic diffusion processes will tend to reduce the influence of initial conditions as $t-t_0$ increases; over extremely long time periods, $t-t_0$, the effect of diffusion (small to medium scale eddies) tends to average out also. It is on the basis of these considerations that Gifford assumes the distribution of material in the instantaneous plume (the function f) to be a fixed function from realization to realization, with parameters varying deterministically with downwind distance and, of course meteorology. Mathematically, Gifford separates the eddies into those which are mixing the plume and those which are moving the plume. In practice, field reports sometimes show plumes having two separate pieces, caused by eddies pulling the plume apart. Thus within an urban-sized area f has a fixed form only in some statistically averaged sense. Nevertheless, if the processes D_y and those contributing to f are independent, then equation (5) still holds. Actually this seems like a good physical assumption, since even though on one realization closely related eddies may both push and tear the plume, such an occurrence is statistically unlikely.

Whatever the actual nature of f , we hypothesize that:

- (a) X is a random variable, due to the stochastic nature of D_y .
- (b) $E\left(\frac{X}{Q_d}\right)$ will be Gaussian a short distance from the source as a consequence of the Central Limit Theorem. (See Appendix B).

Furthermore, if we return from the moving coordinate system and the conceptualization of Figure 1c to the real plume of Figure 1a and the fixed Eulerian viewpoint, we see that the ensemble average of many puffs viewed at the same diffusion times ($t-t_0$) is analogous to averaging the real plume at a fixed downwind position $x = \bar{U}(t-t_0)$ for a significant *finite* averaging time δT (i.e. the Ergodic Theorem holds). It can be demonstrated that $E\left(\frac{X}{Q_d}\right)$ then provides a formal mathematical connection between the instantaneous plume and the time averaged plume.

With f a definite function, then equation (5) is in the form of a convolution transform and we get the result expected for variances of uncorrelated variables:

$$V\left\{E\left(\frac{X}{Q_d}\right)\right\} = V\{f\} + V\{g\} \quad (6)$$

Having assumed that D_y is a random variable forced by the large scale eddies, it is reasonable (Appendix B) to assume that its frequency function, $g(D_y)$, is

Gaussian. This seems to be supported by the available experimental data - as does the Gaussian form for $E\left(\frac{X}{Q_d}\right)$. We can now state the following Lemma: If both $E\left\{\frac{X}{Q_d}\right\}$ and $g(D_y)$ are Gaussian and (5) holds, then f is also Gaussian. The proof follows from the uniqueness of the Weierstrass Transform. This result could have been reached independently by arguing directly that f is Gaussian. This reasoning and some of its experimental implications are clarified in Appendix B.

Having employed the Lagrangian viewpoint and ensemble averages of individual puffs to draw conclusions concerning the nature of E , g and f , Gifford (1959) then returns to the Eulerian representation of a continuous emitting point source of source strength Q and a downwind position $x = \bar{U}(t-t_0)$. f is Gaussian and has the parameter dependence of equation (3). However, initial condition influences are assumed uniform for a continuous emitting point source and in any case have been assumed negligible in deriving the previous results. Consequently,

$$\frac{X}{Q} = \left[2\pi\bar{U}\sqrt{\bar{Y}^2\bar{Z}^2} \right]^{-1} \exp \left\{ -\frac{(y-D_y)^2}{2\bar{Y}^2} - \frac{(z-D_z)^2}{2\bar{Z}^2} \right\} \quad (7)$$

where \bar{Y}^2 is the variance of the material distribution (square of width parameter) in the crosswind direction at $x = \bar{U}(t-t_0)$ and \bar{Z}^2 is the corresponding variance (square of thickness parameter) in the vertical direction. \bar{Y}^2 and \bar{Z}^2 are functions of dispersion time (i.e. x). Since g is Gaussian, equation (7) and equation (5) give:

$$E\left\{\frac{X}{Q}\right\} \equiv \bar{\frac{X}{Q}} = \left[2\pi\bar{U}\sqrt{(\bar{Y}^2+D_y^2)}\sqrt{(\bar{Z}^2+D_z^2)} \right]^{-1} \exp \left\{ \frac{-\bar{Y}^2}{2(\bar{Y}^2+D_y^2)} + \frac{-\bar{Z}^2}{2(\bar{Z}^2+D_z^2)} \right\} \quad (8)$$

where D_y^2 is the variance of $g_1(D_y)$ and D_z^2 is the variance of $g_2(D_z)$.*

*The subscripts "1" and "2" are used here to emphasize that there are now two Gaussian frequency distributions, g , with different variances:

$$g_1(D_y) = \left[2\pi D_y^2 \right]^{-1/2} \exp \left[-y^2/2D_y^2 \right], \quad g_2(D_z) = \left[2\pi D_z^2 \right]^{-1/2} \exp \left[-z^2/2D_z^2 \right].$$

It should be noted that the mean values $E(D_y) = E(D_z) = 0$.

Gifford and other researchers have derived some further properties of this spreading elementary disk fluctuating plume model. The dispersive contributions due to plume spreading (given by $\overline{Y^2}$ and $\overline{Z^2}$) are *statistically independent* of the contributions due to plume meandering (given by $\overline{D_y^2}$ and $\overline{D_z^2}$). Gifford (1959) has observed that the covariance $\overline{YD_y}$ (for the isotropic case) can be shown to be zero. The model formally separates these two aspects of plume dispersion, and in that sense models reality. In real plumes, the independence of spreading and meandering is a general property of dispersion, and is not especially dependent on some peculiarity of the turbulence spectrum or on special meteorological conditions.

Gifford (1960) has also shown, for the case of one-dimensional spreading, that the sum of the mean square dispersion due to spreading of the plume elements and the dispersion of the center of the plume as a result of overall plume fluctuations is equal to the total average dispersion of the plume. Extending the proof to the general case and denoting the total average dispersion of the plume in the crosswind and vertical directions as $\overline{y^2}$ and $\overline{z^2}$ respectively gives:

$$\left. \begin{aligned} \overline{y^2} &= \overline{Y^2} + \overline{D_y^2} \\ \overline{z^2} &= \overline{Z^2} + \overline{D_z^2} \end{aligned} \right\} \quad (9)$$

Following the proof of F. B. Smith (1960), it can also be shown that in the limit of large downwind distances, x :

$$\left. \begin{aligned} \overline{D_y^2} &\rightarrow \text{constant} \\ \overline{D_z^2} &\rightarrow \text{constant} \end{aligned} \right\} \quad (10)$$

At this point, it should be emphasized that the mathematical formalism employed by Gifford (1959, 1960) allows all of the experimental determinations of dispersion coefficients ($\overline{y^2}$ and $\overline{z^2}$) based on time averaging techniques and similar estimates that are routinely used in connection with steady-state plume models to be rigorously interpreted in terms of the fluctuating plume model by means of the formal expected value of the fluctuating plume concentration expression, i.e. the mean concentration distribution of the fluctuating plume (equation(8)). Of immediate interest, is the relation to the non-isotropic dispersion model of Turner (1970) (equation(1)).

In the Turner model, finite ground influences have been taken into account by assuming that *total plume reflection* takes place at the ground and that the resulting concentration $\frac{\bar{X}}{Q}$ can be represented by superposing the concentration distribution of a *fictitious image source* at the position (0,0,-H) in this coordinate system. The coordinate system for Gifford's model is oriented in the same general fashion as in the Turner system, except that the origin (0,0,0) is assumed to be at the effective position of the source and no attempt has been made to include ground effects in his equations. The real effects include deposition and the effects of shear of the mean wind which are not well accounted for by the image source solution, even for the average/steady-state plume. There seems to be no reason why the image source technique cannot be applied to the spreading elementary disk fluctuating plume model for purposes of direct comparison with the Pasquill-Turner average plume model. However, the image source solution is probably even less realistic for the instantaneous plume properties. **

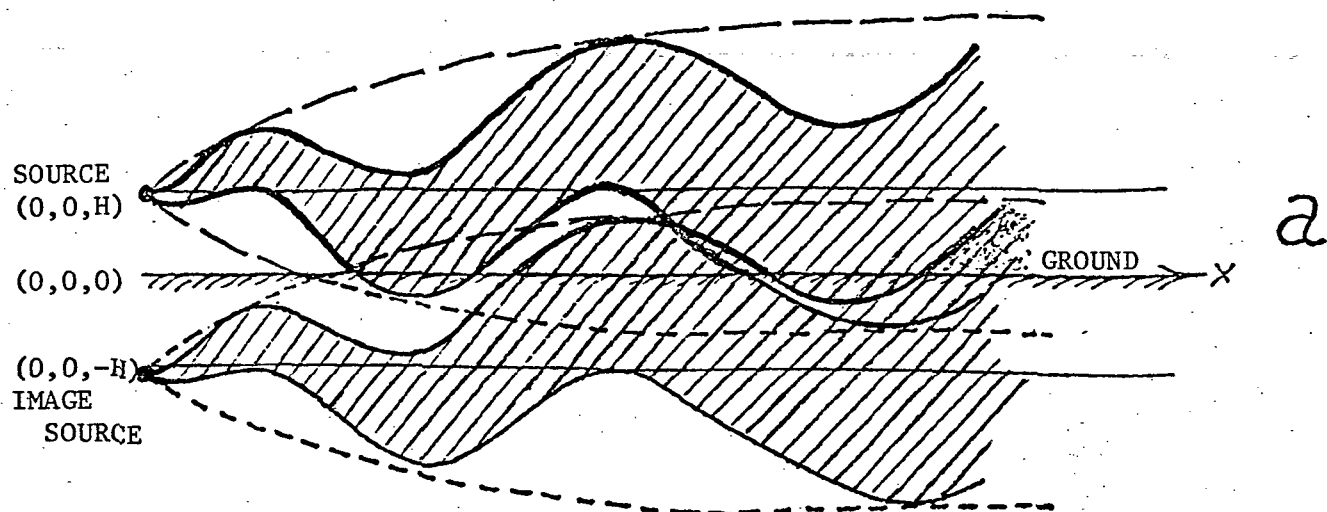
The relation for the steady-state plume concentration in terms of Gifford's coordinate system and neglecting ground influences was given by Pasquill (1962):

$$\frac{\bar{X}}{Q} = \left[2\pi\sigma_y\sigma_z\bar{U} \right]^{-1} \exp \left[-\frac{y^2}{2\sigma_y^2} - \frac{z^2}{2\sigma_z^2} \right] \quad (11)$$

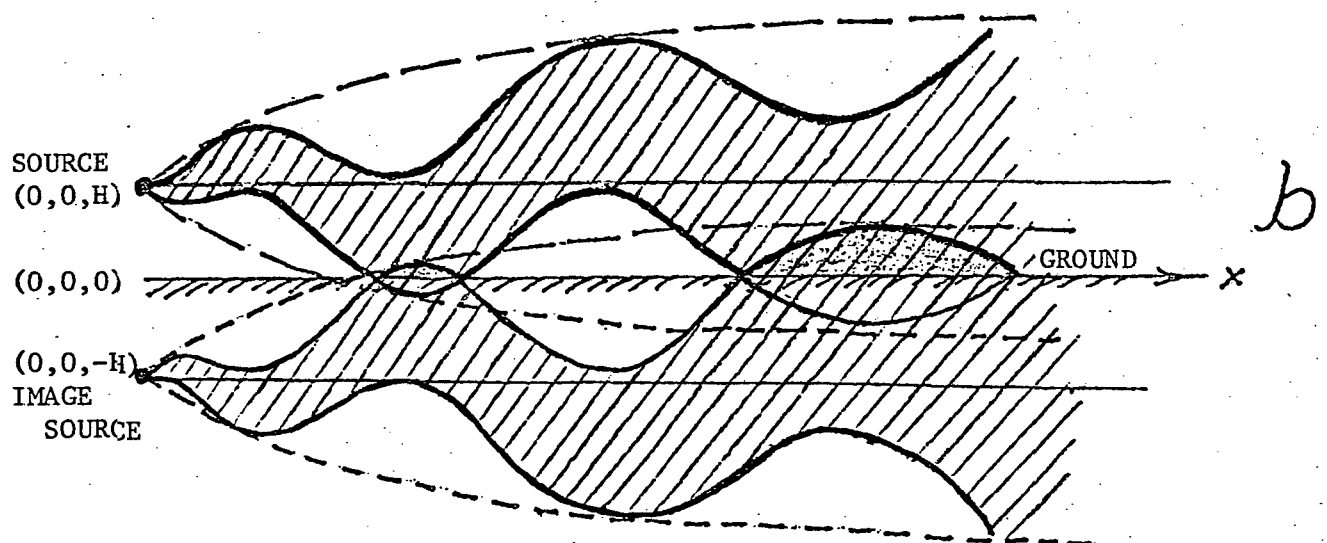
In Turner's expression (equation(1)), the reflection condition at the ground is accomplished by taking the solution for an actual source at position (0,0,H) based on equation (11) and *adding* to this, the solution for a fictitious image source at the position (0,0,-H). Consequently, the exponential term in z in equation (11) is merely replaced by one exponential term in (z-H) and another exponential term in (z+H), leading to equation (1). This technique directly accomplishes reflection only because the Gaussian material distribution of the steady state plume is *symmetric* with respect to the mean plume line.

For the fluctuating plume model, the simple addition of the solutions for sources at altitudes H and -H, as shown in Figure 2a, *will not accomplish reflection* because the asymmetries due to plume meandering must also be reflected in the

** Gifford (1960) notes that the relations for $\frac{\bar{X}(\text{PEAK})}{\bar{X}}$ are probably less seriously affected by ground effects than either X or \bar{X} separately.



INCORRECT APPLICATION OF IMAGE SOURCE



CORRECT APPLICATION OF IMAGE SOURCE

Figure 2. Applications of Image Source to Fluctuating Plume Model

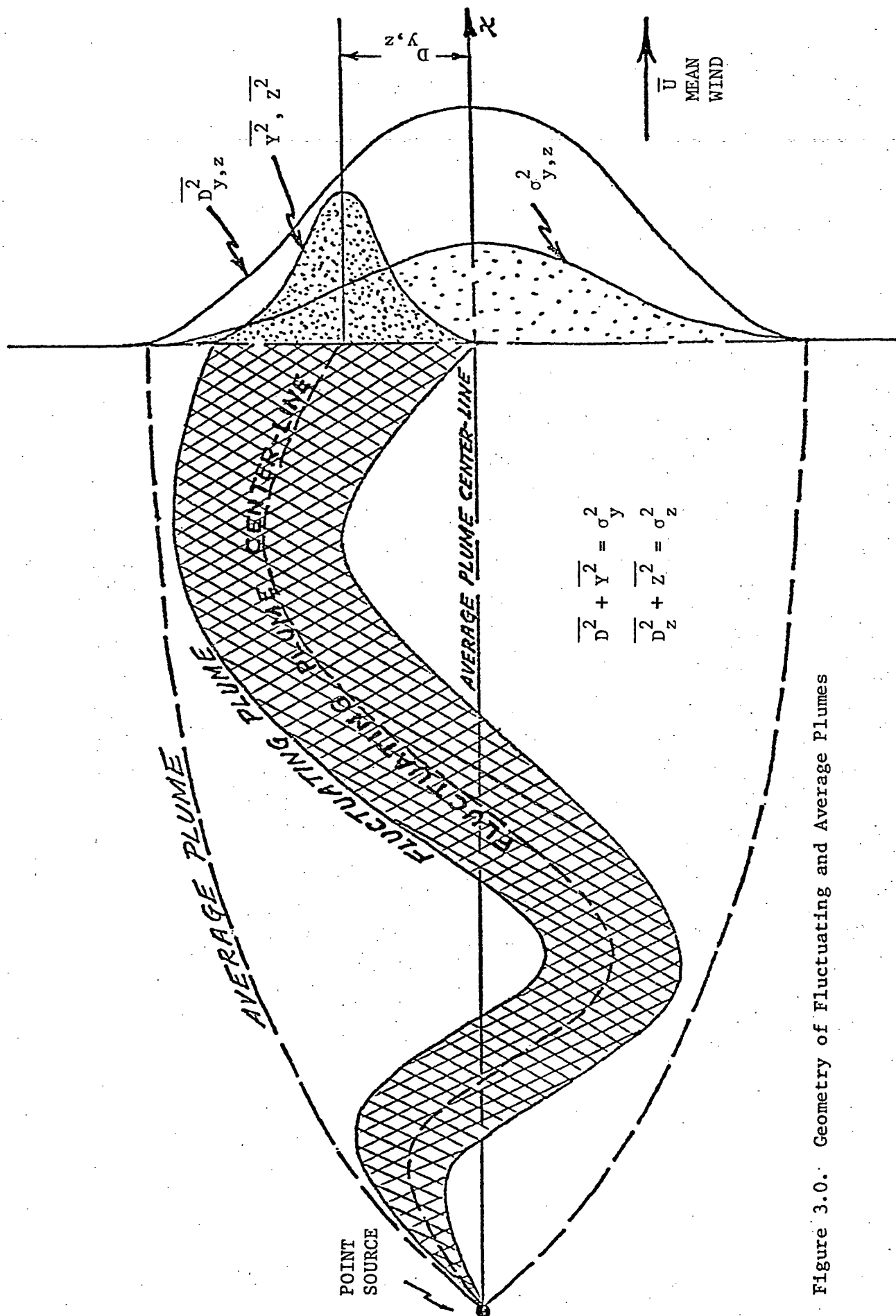
fictitious image source at $-H$. The correct reflection for a fluctuating plume model is illustrated schematically in Figure 2b. With this in mind, equation (7) becomes:

$$\frac{X(x,y,z;H)}{Q} = \frac{1}{2\pi\sqrt{\overline{Y^2}}\sqrt{\overline{Z^2}}\overline{U}} \exp\left\{-\frac{(y-D_y)^2}{2\overline{Y^2}}\right\} \times \left\{ \exp\left[-\frac{(z-H-D_z)^2}{2\overline{Z^2}}\right] + \exp\left[-\frac{(z+H+D_z)^2}{2\overline{Z^2}}\right] \right\} \quad (12)$$

where X is the *instantaneous* pollution concentration. $\overline{Y^2}$ is the variance of the instantaneous concentration of the fluctuating plume in the cross-wind direction, centered about the cross-wind displacement of fluctuating plume, D_y , from the axis of the mean plume (Figure 3.0). $\overline{Z^2}$ is the variance of the instantaneous concentration of the fluctuating plume in the vertical direction, centered about the vertical displacement of the fluctuating plume, D_z , from the axis of the mean plume. The expected value of equation (12) provides the concentration of the time averaged plume:

$$E\left\{\frac{X}{Q}\right\} = \frac{1}{2\pi\sqrt{\overline{Y^2+D_y^2}}\sqrt{\overline{Z^2+D_z^2}}\overline{U}} \exp\left\{-\frac{y^2}{2(\overline{Y^2+D_y^2})}\right\} \times \left\{ \exp\left[-\frac{(z-H)^2}{2(\overline{Z^2+D_z^2})}\right] + \exp\left[-\frac{(z+H)^2}{2(\overline{Z^2+D_z^2})}\right] \right\}, \quad (13)$$

where $\overline{D_y^2}$ is the variance in the cross-wind direction of the frequency distribution of the fluctuating plume centerline displacement from the mean plume axis, i.e. the variance of the frequency distribution of D_y . $\overline{D_z^2}$ is the variance (vertical direction) of the frequency distribution of D_z (Figure 3.0).



Equation (13) is now identified with equation (1)[†] and the variances are related by:

$$\left. \begin{aligned} \sigma_y^2 &= \overline{D_y^2} + \overline{Y^2} \\ \sigma_z^2 &= \overline{D_z^2} + \overline{Z^2} \end{aligned} \right\} \quad (14)$$

One unrealistic approximation of the present model has a self-rectifying tendency. Large amplitude vertical oscillations are inhibited near the ground due to the nature of the rigid boundary, so that treating the lower boundary as a perfect reflector doesn't adequately represent the true situation for the instantaneous plume. This physical representation becomes progressively less realistic with increasing downwind distance as larger scale eddies become dominant. However, as the ratio of the instantaneous plume width to the effective stack height increases with downwind distance, the image source will result in an increasing superposition and "smearing" of the instantaneous material distribution near the ground. The resulting material distribution profile near the ground will consequently have much the same character as for the situation where the large scale vertical oscillations are actually suppressed by the lower boundary.

[†] σ_y^2 and σ_z^2 in equation (1) denote the particular empirical forms of $\overline{y^2}$ and $\overline{z^2}$ developed by Pasquill (1961) and Gifford (1961).

IV. DISPERSION PARAMETER MODELS AND A PRIORI INFORMATION

The plume models described in Section III represent only a portion of the modeling required for dispersion simulation and estimation. In this section, the modeling of the specific plume parameters appearing in equations (1), (12) and (13) will be addressed, including the stochastic properties of the fluctuating plume which are manifested through the parameters D_y and D_z of equation (12).

The parameters appearing in equations (1), (12) and (13) fall into three categories:

- A. *Source Related Parameters,*
 $Q, x_0, y_0.$
- B. *Meteorological Related Parameters,*
 $\bar{U}, \theta, \sigma_y^2, \sigma_z^2, D_y, D_z, D_y^2, D_z^2, Y^2, Z^2.$
- C. *A Combination of Source and Meteorological Parameters,*
 $H.$

The quantity H may be written as

$$H = H_0 + \Delta H \quad (15)$$

where H_0 is the physical stack height (a source related parameter) and ΔH is the plume rise (a combination of source and meteorological parameters).

In addition, *a priori* estimates of the various plume parameters will be considered. All of the above parameters have some *a priori* estimates and associated uncertainties. The present section is concerned with the functional forms and *a priori* estimates of the class of meteorological related parameters. Of these, we will not be concerned with the wind parameters (\bar{U}, θ) at the present time, but will consider the remaining *dispersion parameters* $(\sigma_y^2, \sigma_z^2, D_y, D_z, D_y^2, D_z^2, Y^2, Z^2).$

Utilization of *a priori* knowledge alone in conjunction with plume models corresponds to the usual application of air pollutant dispersion simulation. The optimum combination of *a priori* knowledge and air quality measurements in conjunction

with plume models through a systematic parameter estimation procedure to provide improved air pollutant dispersion simulations is the ultimate objective of the current research effort.

It should be noted at this point, that the considerations provided in the present section concerning *a priori* values of plume parameters and the associated uncertainties are not to be considered as fixed aspects of the model. Just as in the application of models without an estimation algorithm, the experience of a meteorologist in assigning input values and estimates of their true uncertainties for a specific set of topographical and meteorological conditions can greatly improve the model predictions. However, the estimation algorithm will, *in addition*, utilize the appropriate mathematical expression of the uncertainties in the *a priori* information to properly weight the best first estimate of all parameters with the additional information implicit in air quality measurements to provide a new, updated estimate.

Variances of the Average Plume Concentration Distribution, σ_y^2 and σ_z^2

The vast majority of published continuous plume dispersion data relate to the variances of the *average* plume material distribution σ_y^2 and σ_z^2 . In contrast to the average plume dispersion parameters, published observational data on *instantaneous* fluctuating plumes are scarce. A similar situation prevails with respect to theoretical results. Of the two variances, σ_y^2 and σ_z^2 , more is known about σ_y^2 . In the first place, more observational data is available since ground level networks supply an adequate measure of the σ_y^2 properties but instrumented tower, airborne measurements or recently developed remote sensing techniques are required to study the characteristics of σ_z^2 . Also, theoretical study of σ_z^2 is complicated by the influences of the lower boundary at the ground, the upper boundary provided by a stability layer of some kind and the buoyancy properties of the atmosphere.

Observational data suggest that the horizontal standard deviation has the functional form (Slade, 1968):

$$\sigma_y^2(x) = (\sigma_y^0)^2 x^{2p} , \quad (16)$$

with

$$p = 0.85 + \delta = \text{Constant} , \quad (17)$$

where the constants σ_y^0 and p , are dependent on the conditions of atmospheric stability. The observations fit equation (16) very well over the range 50 meters $\leq x \leq$ 50 kilometers. In addition, a variety of long range measuring techniques suggest that equation (16) may hold through the range 10 kilometers $\leq x \leq$ 10^4 kilometers (Heffter, 1965; Slade, 1968). There is some indication that δ may be a weak function of atmospheric stability (i.e. temperature structure), particularly for highly stable conditions. For stable conditions, $-0.4 \leq \delta \leq 0$. σ_y^0 , on the other hand, is known to be strongly dependent upon atmospheric stability.

Pasquill (1961) and Gifford (1961) using observational data and theoretical considerations have provided values for the coefficients appearing in equation (16), based on standardized atmospheric stability categories. The results, given for the range 100 meters $\leq x \leq$ 100 kilometers, are available in graphical form in Turner (1970). All the σ_y curves in Turner (1970) are based on $\delta = 0.053$. The results were derived on the basis of a sampling time of about 10 minutes. Potential complications arising from application of measurements taken by instruments with different *non-instantaneous* averaging times in different regions of the plume will be considered in Section V.

The *a priori* value of σ_y^0 may be taken from Turner's curves, as a function of Pasquill atmospheric stability category, with some uncertainty (taken as ± 1 stability category in the absence of more specific estimates). Since p does not appear to decrease below 0.45 (Slade, 1968) even for the most stable atmospheric conditions (which are not expected to occur for urban conditions in any case) and does not appear to exceed the theoretical limit of 1.0 even for the most extreme conditions of instability, the range of δ (equation (17)) may be taken as:

$$-0.40 \leq \delta \leq + 0.15 . \quad (18)$$

Observational data suggests that the vertical standard deviation can be generally represented by the functional form (Slade, 1968):

$$\left. \begin{aligned} \sigma_z(x) &= \sqrt{\sigma_z^2} = \sigma_z^0 x^q, \\ \text{or in terms of the variance:} \\ \sigma_z^2(x) &= (\sigma_z^0)^2 x^{2q} \end{aligned} \right\} \quad (19)$$

where σ_z^0 is a function of the atmospheric stability condition. Unlike "p" in equation (16), however, q is both a function of atmospheric stability condition and of the downwind distance from the source:

$$q = q(x) .$$

Pasquill (1961) and Gifford (1961) have provided values of $\sigma_z(x)$ as a function of atmospheric stability. Turner (1970) has presented the results graphically by atmospheric stability category. The exponent $q(x)$ for these six stability classes as markedly different behavior for stable and unstable conditions.

Turner's curves do not include the most stable conditions that occur in the atmosphere. In these situations, the plume may exhibit only the slowest regular vertical dispersion while the horizontal growth is dominated by the characteristic sinuous meandering of the instantaneous plume, i.e. the situation known as *fanning* (Slade, 1968). In this case, we would expect:

$$q(x) \rightarrow \text{constant} \ll 1, \text{ as } x \rightarrow \infty . \quad (20)$$

In practice, many operational urban air pollution simulations have represented $\sigma_z(x)$ by equation (19) (Koch and Thayer, 1971; McElroy and Pooler, 1968), or by the similar form (Calder, 1970):

$$\sigma_z(x) = \sigma_z^0 x^q + \sigma_z^1 . \quad (21)$$

In either case, $\sigma_z(x)$ is given as a piecewise continuous function with $q(x)$ being a different constant for different downwind regions. This is not necessarily the most convenient way of representing $q(x)$ for estimation purposes, since the downwind distance from the source may also be one of the quantities to be estimated. For estimation purposes, the $q(x)$ curves for different stability conditions and the condition of equation (20) can all be approximated by the family of curves:

$$q(x) = q_0 + q' \exp(-\lambda x) , \quad (22)$$

where q_0 , q' and λ are functions of atmospheric stability *but are not functions of x* . $q_0 > 0$ for all stability conditions, but $q' \approx 0$ for neutral stability, $q' > 0$ for unstable conditions and $q' < 0$ for stable conditions. For small x , $q(x) \rightarrow q_0 + q'$ and for large x , $q(x) \rightarrow q_0$. For the case of neutral stability, if the slight curvature in Turner's curve is neglected, then $q(x) \approx q_0 \approx 0.911$. The values of the coefficients appearing in equation (22) have been obtained by a numerical least squares fit to Turner's curves. These values are given in Table 1, and can be used as *a priori* values for the given stability classes, with an uncertainty of ± 1 stability class (in the absence of better meteorological estimates).

TABLE 1
A PRIORI VALUES OF COEFFICIENTS FOR σ_y (METERS)
AND σ_z (METERS) BASED ON NUMERICAL FIT OF THE
 σ_z PASQUILL-GIFFORD DATA AS PRESENTED
BY TURNER (1970)

Pasquill-Turner Stability Class	σ_y^0	P	σ_z^0	q_0	q'	$\lambda \times 10^3$
A	0.400	0.903	0.000186	2.13	0.749	8.73
B	0.295	0.903	0.0560	1.10	0.105	8.74
C	0.200	0.903	0.107	0.918	0.00164	6.55
D	0.130	0.903	0.385	0.638	-0.159	5.11
E	0.098	0.903	0.428	0.570	-0.162	4.30
F	0.066	0.903	0.432	0.511	-0.194	3.58

The power function relation of equation (19) for $\sigma_z(x)$ and the associated coefficients are only valid when there is unrestricted diffusion in the vertical direction above the ground. Frequently, a stable region of the atmosphere or

inversion layer, will exist at some altitude L . Vertical diffusion is then strongly inhibited for $z > L$ and the dispersing pollutants tend to be trapped in the region $z \leq L$. The region $z \leq L$ is known as the *mixing layer*.

We will employ the concept, based on the proposal of Pasquill (1962), of representing the effect of the upper boundary in terms of the standard deviation of the mean plume, rather than in terms of the form of the concentration expression. It will also be assumed that the effect of a mixing layer must eventually cause the vertical dispersion to approach a uniform distribution at some distance x_u far enough downwind. However, the statement of this concept employed by Pasquill (1962), that

$$\sigma_z(x_u) = L \quad (23)$$

is not necessarily the best way of approximating this situation in terms of the Gaussian plume model for purposes of estimation theory applications with measurement data.

If the form of the Gaussian plume is to be retained, then the thickness parameter σ_z of the vertical concentration distribution $V_1(x, z; H)$ based on equation (1) for uniform mixing given by:

$$V_1(x, z; H) = \frac{1}{\sqrt{2\pi} \sigma_z \bar{U}} \left\{ \exp \left[-\frac{1}{2} \left(\frac{z-H}{\sigma_z} \right)^2 \right] + \exp \left[-\frac{1}{2} \left(\frac{z+H}{\sigma_z} \right)^2 \right] \right\}, \quad (24)$$

is the only free parameter which may be used to fit the Gaussian to the uniform vertical distribution given by:

$$V_u(z) = \begin{cases} \frac{1}{\bar{U}L} & , \quad 0 \leq z \leq L \\ 0 & , \quad z > L \end{cases} \quad (25)$$

The Pasquill relation (equation (23)) provides one means of fitting the two distributions. However, this will result in a fairly large proportion of the area of V_1 being above the mixing layer, $z = L$. This will probably provide a satisfactory approximation for application with ground based measurements or remote measurements from high altitude platforms, but will result in considerable departure from concentrations predicted by the uniform distribution for altitudes corresponding to

measurements taken by airborne grab samplers or measurements recorded from tall buildings or towers. On the other hand, the V_1 distribution can be required to lie below the altitude $z = L$ out to the $3\sigma_z$ level, i.e.:

$$3\sigma_z(x_u) = L \quad (26)$$

This will result in a large departure from the concentrations predicted by the uniform distribution near the ground, which is undesirable for application with ground measurements.

A method for matching the two distributions, which provides an overall compromise for the requirements of a wide range of measurement types, involves matching the second moment σ_V^2 of the V_1 distribution to the second moment v_z^2 of the uniform distribution V_u . Consider the case, $H < L$, then approximate this by $H \approx 0$, i.e.:

$$V_1(x, z; 0) = \frac{1}{U} \sqrt{\frac{2}{\pi\sigma_z^2}} \exp \left[-\frac{1}{2} \left(\frac{z}{\sigma_z} \right)^2 \right], \quad (27)$$

the second moment of $V_1(x, z; 0)$ about $z = 0$ is:

$$\sigma_V^2 = \int_0^\infty z^2 V_1(x, z; 0) dz = \frac{\sigma_z^2}{U} \quad (28)$$

The second moment is of V_u about $z = 0$ is:

$$v_z^2 = \int_0^L z^2 V_u dz = \frac{1}{UL} \int_0^L z^2 dz = \frac{L^2}{3U} \quad (29)$$

The condition for fitting V_1 to V_u is then:

$$\sigma_z(x_u) = \frac{L}{\sqrt{3}} \quad (30)$$

Using the power law for σ_z ,

$$x_u = \left(\frac{\sigma_u(L, 0)}{\sigma_z^0} \right)^{1/q(x_u)} \quad (31)$$

where

$$\sigma_u(L, 0) = L/\sqrt{3} \quad (32)$$

unless noted otherwise.

We will assume that the power law (equation 18) is valid up to some position x_L where the effects of the mixing layer are first felt. Turner (1970) observed that for the situation where $H \ll L$, letting $H \rightarrow 0$ in equation (1), then for $z_0 = 2.15\sigma_z$:

$$\bar{X}(x, y, z_0; 0) = 10^{-1} \bar{X}(x, y, 0; 0) \quad (33)$$

When $L = 2.15\sigma_z$, it is then assumed that this situation represents the first instance where the elevated stable layer or "lid" begins to influence the vertical distribution of pollutants. Let the position x where this occurs be x_L :

$$\sigma_z(x_L) = \frac{L}{2.15} = 0.47L \quad (34)$$

Then, the value of x_L is obtained by assuming that the power law, equation (18), is valid up to x_L , so that:

$$x_L = \left(\frac{0.47L}{\sigma_z^0} \right)^{1/q(x_L)} \quad (35)$$

$$q(x_L) = q_0 + q \exp(-\lambda x_L) \quad ,$$

For $x < x_u$ equation (31) holds, and for $x_L \leq x \leq x_u$, an interpolation scheme will be employed. In order to avoid having σ_z defined differently for different down-wind regions, the linear interpolation will not be employed. Instead, we will employ the function which accomplishes very much the same thing but is continuous for all x :

$$\left. \begin{aligned} I(x) &= \frac{1}{2} \left\{ 1 + \tanh \left[\frac{2(x - \bar{x})}{x_u - x_L} \right] \right\} \\ \bar{x} &= \frac{x_u + x_L}{2} \end{aligned} \right\} \quad (36)$$

Finally we have:

$$x_L = \left(\frac{0.47L}{\sigma_z^0} \right)^{1/q(x_L)} \quad , \quad x_u = \left(\frac{\sigma_u(L, 0)}{\sigma_z^0} \right)^{1/q(x_u)} \quad (37)$$

where $\sigma_u(L, 0)$ is given by equation (32), unless noted otherwise. It should be noted that

we could well have applied our interpolation function directly to \bar{x} to blend the Gaussian plume into the vertical uniform distribution. However, in the process we introduce the mixing layer influence into a "higher level" of the model with subsequent expanded influence in the sensitivity calculations, i. e. many more partial derivatives are then affected.

$$q(x) = q_0 + q \exp(-\lambda x) \quad (38)$$

$$I(x) = \frac{1}{2} \left\{ 1 + \tanh \left[\frac{2(x-\bar{x})}{x_u - x_L} \right] \right\} \quad (39)$$

$$\bar{x} = \frac{x_u + x_L}{2} \quad (40)$$

$$\sigma_z^2(x) = \left[\sigma_z^0 q (1-I(x)) + \sigma_V^* I(x) \right]^2 \quad (41)$$

$$\sigma_V^* = \sigma_u(L, H) \left[1 - \exp \left(- \frac{10.0x}{x_L} \right) \right] \quad (42)$$

$$\sigma_u(L, H) \approx \sigma_u(L, 0), \quad H \ll L \quad (43)$$

where

$$\sigma_u(L, 0) = \frac{L}{\sqrt{3}} \quad (44)$$

unless noted otherwise. σ_V^* is virtually constant for $x > x_L$ and equals zero when $x = 0$. This property guarantees $\sigma_z^2(0) = 0$ which otherwise would not be the case for an asymptotic interpolation function. The exponential in equation (42) guarantees that $\sigma_V^* = 0$ at $x = 0$ with a smooth transition to $x = x_L$.

The technique employed above for fitting V_1 to V_u by matching second moments was selected to provide a good fit for the widest range of measurement types. However, for a given measurement scenario, other matching criteria may be more suitable. We have already mentioned Pasquill's criteria, given by equation (23) and the condition for maintaining most of the area of V_1 below the mixing layer, given by equation (26). Other possible criteria include: (a) matching the first moments of V_1 and V_u about $z = 0$, i.e. matching the means; (b) matching the medians of V_1 and V_u , i.e. requiring V_1 to have equal area below and above the altitude $z = L/2$; (c) Providing an overall least squares fit of V_1 to V_u ;

(d) matching the ground concentration provided by V_1 to the value given by V_u ;
 (e) minimizing the areas of *mismatch* between V_1 and V_u near the ground *and* above the mixing layer $z = L$; (f) minimizing the total area of *mismatch* between V_1 and V_u for all altitudes $z \geq 0$. This condition can be shown to be equivalent to (e) above for all practical purposes.

The results for the limiting values of the width parameters $\sigma_u(L, H)$ under the assumption that $L \gg H$ (i.e. $\sigma_u(L, 0)$) and the corresponding ground concentration $V_1(x_u, 0; H=0)$ are summarized in Table 2.

TABLE 2
 LIMITING VALUES OF THE GROUND CONCENTRATION AND THICKNESS
 PARAMETER σ_u OBTAINED BY MATCHING V_1 TO V_u
 UNDER THE ASSUMPTION THAT $L \gg H$

Matching Criteria	$\sigma_u(L, 0)/L$	$V_1(x_u, 0; 0)/V_u(0)$
1. Pasquill's Criteria $\sigma_u = L$	1	0.7979
2. $3\sigma_u$ at the mixing layer, $z = L$	0.3333	2.394
3. Matching second moments about $z = 0$	0.5774	1.382
4. Matching means	0.6267	1.273
5. Matching medians	0.7414	1.076
6. Least squares fit	0.6935	1.151
7. Matching ground concentrations	0.7979	1
8. Minimizing area of mismatch wear $z = 0$ and above $z = L$	0.6728	1.186
9. Minimizing total area of mismatch for $z \geq 0$	0.6730	1.186

Variances of the Instantaneous Plume Centerline Distributions, $\overline{D_y^2}$ and $\overline{D_z^2}$

As previously observed, the state of theoretical and observational knowledge of the fluctuating plume parameters is rather limited. One set of fluctuating plume parameters is the crosswind and vertical variances, $\overline{D_y^2}$ and $\overline{D_z^2}$, of the frequency distribution of the instantaneous plume centerline displacement with respect to the mean plume axis.

One definite constraint on the functional behavior of $\overline{D_y^2}(x)$ and $\overline{D_z^2}(x)$ with downwind distance is given by equation (14). Also, since the instantaneous plume thickness never vanishes, $Y^2(x) > 0$ and $Z^2(x) > 0$. Hilst (1957) measured the variances of the instantaneous and average plumes for very stable atmospheric conditions and for distances less than one kilometer from the source. He found that the power law:

$$\overline{D_y^2} = \overline{D_{y0}^2} x^{2P} \quad , \quad (45)$$

where $\overline{D_{y0}^2}$ is a constant, satisfied his observations very well. For almost all of his observations, he found that $\overline{D_y^2}$ contributed one half or more of the total variance, σ_y^2 and that these instances divided about equally between the situations $\overline{D_y^2} \approx \frac{\sigma_y^2}{2}$ and $\overline{D_y^2} \gg \frac{\sigma_y^2}{2}$. In any case, the implication is that for the range of x considered, $\overline{D_y^2} \sim \sigma_y^2$. From equations (16) and (17), this implies that $\frac{1}{2}(\sigma_y^0)^2 \leq \overline{D_{y0}^2} < (\sigma_y^0)^2$, and that the *a priori* value of $\overline{D_{y0}^2}$ is $\sim \frac{1}{2}(\sigma_y^0)^2$. Similarly equations (16) and (17) imply that $P \sim p \sim 1.0$.

Since the width of the instantaneous plume can never equal zero for $x > 0$, we know that $\overline{D_{y0}^2} \leq (\sigma_y^0)^2$ for all $x > 0$. However, it is clear from equations (10), (16) and (17) that Y^2 must eventually predominate at large downwind distances, so that if equation (45) were to hold to all $0 \leq x < \infty$, then equation (10) would require $P = P(x) \rightarrow 0$, $x \gg 1$. Since the fluctuations characterized by D_y are of amplitude determined by the range of turbulent eddies whose scale is proportional to the distance from the source (Section II) up to some limiting scale, we would further expect $\overline{D_y^2}$ to be a monotone increasing function of x .

Very little is known about the actual limiting value, $\overline{D_y^2} \rightarrow \overline{D_{y\infty}^2}$, or the downwind distance x_∞ at which this situation approximately prevails. However, theoretical considerations concerning the instantaneous and average peak concentration values (Gifford 1959, 1960) suggest that:

$$\frac{X(\text{PEAK})}{\overline{X}(\text{PEAK})} \rightarrow 1, \quad x \rightarrow x_\infty.$$

The few measured values of this ratio that are available (Gifford, 1960) suggest that x_∞ probably exceeds the 1-10 kilometer range. Whereas, the available observations (Hilst, 1957) suggest that the power law (equation 45) is reasonable to distances of about one kilometer, at least.

Let $x = x_p$ be the hypothetical distance at which the power law would yield the value $\overline{D_y^2} = \overline{D_{y\infty}^2}$, if it were to hold that far downwind:

$$x_p = \left\{ \sqrt{\frac{\overline{D_{y\infty}^2}}{\overline{D_{y0}^2}}} \right\}^{1/P} \quad (46)$$

Assume that the power law is approximately valid out to a distance $x \leq \frac{1}{2}x_p$. Furthermore, let the actual limit $\overline{D_{y\infty}^2}$ be approximately achieved (to the 95% level or better) at a distance $x = 2x_p$. Let the $\overline{D_y^2}$ relation provide a smooth monotone transition in the range $\frac{1}{2}x_p \leq x \leq 2x_p$. A functional form which satisfies these requirements is:

$$\overline{D_y^2}(x) = \overline{D_{y0}^2} \left\{ x_p \tanh\left(\frac{x}{x_p}\right) \right\}^{2P} \quad (47)$$

We will take 1-50 kilometers as the assumed range of x_p with an *a priori* value of 10 kilometers. The *a priori* value of $\overline{D_{y\infty}^2}$ will be obtained by setting $x = 10$ km (10^4 meters) in equation (45) with the *a priori* values of $P \approx p = .903$ and $\overline{D_{y0}^2} = \frac{1}{2}(\sigma_y^0)^2$ from Turner's graphical values of σ_y . The range of $\overline{D_{y\infty}^2}$ can be obtained by taking the upper and lower limits of the range x_p and the upper and lower limits on the range of p from equations (17) and (18). $\overline{D_{y0}^2}$ is, of course, a function of atmospheric stability category with some uncertainty, say ± 1 stability category.

Hilst's observations (Hilst, 1957) provided no information on $\overline{D_z^2}$, since for the highly stable conditions of his experiments, the plume spreads very gradually in the vertical direction with no evidence of vertical meandering, so that $\overline{D_z^2}(\text{stable}) \approx 0$. Since both crosswind and vertical meandering are a result of the turbulent eddy motion, we can expect atmospheric stability, the presence of an upper boundary (mixing height) and a lower boundary (ground) to produce effects analogous to their influence on σ_z^2 .

By analogy with $\overline{D_y^2}$, let us assume that the power law:

$$\overline{D_z^2}(x) = \overline{D_{z0}^2} x^{2Q} \quad (48)$$

holds for $x < \frac{x'_p}{2}$. Let $\overline{D_{z\infty}^2}$ be the theoretical limit of equation (10). Then:

$$x'_p = \left\{ \sqrt{\frac{\overline{D_{z\infty}^2}}{D_{z0}^2}} \right\}^{1/Q(x'_p)} \quad (49)$$

and,

$$\overline{D_z^2}(x) = D_{z0}^2 \left\{ x'_p \tanh\left(\frac{x}{x'_p}\right) \right\}^{2Q} \quad (50)$$

in the absence of an upper boundary. By analogy with Hilst's observations for $\overline{D_y^2}$, we will assume an *a priori* value for $\overline{D_{z0}^2} = \frac{1}{2}(\sigma_z^0)^2$ for all stability categories. For stable conditions, the *a priori* value of $\overline{D_{z0}^2}$ is very small.

By analogy with $\overline{D_y^2}$ and σ_z^2 , we will assume that:

$$Q = Q(x) = Q_0 + Q' \exp\{-\Lambda x\}, \quad (51)$$

with *a priori* values $Q_0 \approx q_0$, $Q' \approx q'$, $\Lambda \approx \lambda$, from equation (22), i.e. $\overline{D_z^2}$ follows approximately the same power law as σ_z^2 for $x \leq x'_p/2$. The discussion concerning the *a priori* values of $q(x)$ then applies to $Q(x)$. For very stable conditions, however, $\overline{D_z^2}(x) \approx \overline{D_{z\infty}^2} \approx \overline{D_{z0}^2}$ are very small. Then, $Q' \approx -Q_0$, $Q_0 \approx q_0$, $\Lambda \approx 0$. Therefore, we set $Q(x) \rightarrow \text{constant} \approx 0$ as $x \rightarrow \infty$ in the very stable case.

The situation where a mixing layer of thickness L is present can be formulated in a convenient manner directly in terms of the concentration, if we assume that the presence of the layer eventually causes complete mixing in the vertical direction so that the mean plume is represented as having a uniform vertical distribution. We can extend the idea to the instantaneous plume by assuming that local vertical meanderings and fluctuations are not really distinguishable in the case of uniform mixing, so that the instantaneous vertical distribution is the same as the mean vertical distribution, i.e. uniform. However, for estimation purposes, it is desirable to leave the form of the concentration equation unaltered, and to express the effects of the mixing layer thru the vertical diffusion parameters. Expressing the effects of the mixing layer in terms of the vertical diffusion parameters of the fluctuating plume model, $\overline{D_z^2}$ and Z^2 , without altering

the basic instantaneous concentration expression, (equation (12)) presents a more complicated problem.

In the presence of a mixing layer of thickness \bar{L} , $\bar{D}_z^2(x)$ will approach a constant value \bar{D}_{zL}^2 , such that $\bar{D}_{zL}^2 \leq \bar{D}_{z\infty}^2$. If $\bar{D}_{zL}^2 = \bar{D}_{z\infty}^2$, the mixing layer is too high to have any effective influence on the vertical meandering of the plume before it becomes self-limited. The mixing layer effects are then felt through σ_z^2 and Z^2 , since Z^2 has become dominant over \bar{D}_z^2 under these circumstances. We can also expect that $0 < \bar{D}_{zL}^2$, since the scale of turbulent eddies which determine $\bar{D}_{z\infty}^2$ are not expected to be particularly suppressed by the upper boundary of the mixing layer, and in fact should contribute to the "mixing" associated with the layer. In this case, $\bar{D}_z^2(x)$ may be represented by:

$$\bar{D}_z^2(x) = \bar{D}_{z0}^2 \left\{ x'_p \tanh\left(\frac{x}{x'_p}\right) \right\}^{2Q} \quad (52)$$

$$x'_p = \left\{ \sqrt{\frac{\bar{D}_{z0}^2}{\bar{D}_{z\infty}^2}} \right\}^{1/Q(x'_p)} \quad (53)$$

We will take 1-50 kilometers as the assumed range of x'_p , with an *a priori* value of 10 kilometers. $Q(x)$ is given by equation (51), with an *a priori* value $Q(x) \approx q(x)$ of equation (22) with the associated *a priori* values of (q_0, q', λ) for the given stability condition (these values themselves have an uncertainty, taken to be about ± 1 stability category). The *a priori* value of $\bar{D}_{z0}^2 = \frac{1}{2}(\sigma_z^0)^2$ for the given stability condition (again uncertain to say ± 1 stability category). The *a priori* value of $\bar{D}_{z\infty}^2$ will be obtained by setting $x = 10\text{km}$ (10^4 meters) in the power law, equation (48). The range $\bar{D}_{z\infty}^2$ can be obtained by taking the upper and lower limits of the ranges of x'_p , $Q(x'_p)$, \bar{D}_{z0}^2 in equation (48).

If $\bar{D}_{zL}^2 \leq \bar{D}_{z\infty}^2$, then we are concerned with a situation where Z^2 does not yet dominate \bar{D}_z^2 when the effects of the vertical "lid" are felt. In that case, the mixing layer influences the limiting value of \bar{D}_z^2 and probably the way that limit is approached. We assume that the critical distances involved are the same as those defined for σ_z^2 , so that we may expect relations corresponding to equations (37)-(44) will be valid:

$$x_L = \left(\frac{0.47L}{\sigma_z^0} \right)^{1/q(x_L)}, \quad x_u = \left(\frac{\sigma_u(L,0)}{\sigma_z^0} \right)^{1/q(x_u)} \quad (54)$$

$$q(x) = q_0 + q' \exp(-\lambda x) \quad (55)$$

$$I(x) = \frac{1}{2} \left\{ 1 + \tanh \left[\frac{2(x - \bar{x})}{x_u - x_L} \right] \right\} \quad (56)$$

$$\bar{x} = \frac{x_u + x_L}{2} \quad (57)$$

$$\overline{D_z^2}(x) = \left[\sqrt{D_{z0}^2} x^Q \{1 - I(x)\} + \sqrt{D_{zL}^2} \left\{ 1 - \exp \frac{-10.0x}{x_L} \right\} I(x) \right]^2 \quad (58)$$

$$Q(x) = Q_0 + Q' \exp(-\lambda x) \quad (59)$$

where equations (54)-(57) are identical to the corresponding σ_z relations. We may note that $\frac{1}{2}\sigma_u^2(L,H) \leq D_{zL}^2 < \sigma_u^2(L,H)$, with an *a priori* value of $D_{zL}^2 = \frac{1}{2}\sigma_u^2$. The *a priori* values for the other parameters appearing in equation (54)-(59) have been discussed previously.

The remaining question concerns the criteria for selecting the particular $\overline{D_z^2}$ functional form for estimation purposes in the presence of a mixing layer. A possible selection criterion is to use relations (55)-(59), whenever the natural limit $\overline{D_z^2}^\infty$ would be reached (according to the power law, equation (45)) well after

the effects of the "lid" are felt, i.e. whenever $x'_p > x_L$. Equivalently, whenever:

$$L^2 < 4.53(\sigma_z^0)^2 \left[\frac{\overline{D_{z\infty}^2}}{\overline{D_{z0}^2}} \right]^{q/Q} \quad (60)$$

In practice, the decision will be made in terms of the *a priori* values, so that equation (60) becomes:

$$L < 3\sqrt{\overline{D_{z\infty}^2}} \approx \frac{3\sqrt{2}}{2} \sigma_z^0 10^{4q_0} \text{(meters)} \quad (61)$$

Variances of the Instantaneous Plume Material Distribution, $\overline{Y^2}$ and $\overline{Z^2}$

For large distances x , Batchelor (1950) has shown that $\overline{Y^2}(x)$ must become independent of two particle statistics. As a consequence, $\overline{D_y^2}$ must approach a constant far downwind (see previous discussion in this section) and $\overline{Y^2}$ varies as σ_y^2 , which is dictated by a power law. Hilst (1957) found that observations of $\overline{Y^2}$ under most stable conditions for distances $x \leq 1$ km were very well predicted by the power law. Consequently, for all x , the power law:

$$\overline{Y^2}(x) = \overline{Y_0^2} x^{2P} \quad (62)$$

can be expected to provide a reasonable approximation. As previously noted, Hilst's observations indicated that meandering effects either dominated the relative diffusion effects or contributed about equally, so that $P \sim P_p$ and $0 < \overline{Y^2} \lesssim \frac{1}{2}\sigma_y^2$.

Theoretical considerations and observations for neutral stability conditions (Högström, 1964) indicate for small x , that $\overline{Y^2} \sim \frac{1}{2}\sigma_y^2$ when σ_y^2 is determined for averaging times on the order of tens of minutes. Consequently, the *a priori* value of $\overline{Y_0^2}$ can be taken to be $\frac{1}{2}(\sigma_y^0)^2$. If equation (14) is to be observed in strict equality then $\overline{Y_0^2}$ must actually be a weak function of x , i.e.:

$$\overline{Y_0^2} = \frac{1}{2}(\sigma_y^0)^2 \left[2x^{2(p-P)} - \frac{2D_{y0}^2}{(\sigma_y^0)^2} \left\{ x_p \tanh\left(\frac{x}{x_p}\right) \right\}^{2P} x^{-2P} \right] \quad (63)$$

The expected value of the quantity in brackets in (63) is in fact ≈ 1 for $x \leq \frac{x_p}{2}$.

With respect to $\overline{Z^2}$, observations (Högström, 1964) for neutral stability conditions and small downwind distances indicate that $\overline{Z^2} \sim \frac{1}{2}\sigma_z^2$. Hilst (1957) made observations of σ_z^2 under very stable atmospheric conditions, so that vertical meandering was almost completely suppressed and $\sigma_z^2 \sim \overline{Z^2}$. His observations were limited in extent, but indicated that $\overline{Z^2}$ initially followed a power law:

$$\overline{Z^2} = \overline{Z_0^2} x^{2Q'} \quad (64)$$

but leveled out so that $\sigma_z^2 \sim \overline{Z^2} \rightarrow \text{constant}$, for $x > 300\text{m}$. These observations do not contradict equation (14) with the functional form and *a priori* values prescribed by σ_z^2 and $\overline{D_z^2}$.

Since the very little theoretical or observational information that is available concerning the behavior of the variances of the instantaneous relative plume material distribution as a function of downwind distance, is not in conflict with the constraint condition provided by equation (14) with the functional forms and *a priori* values already formulated for the pairs (σ_y^2, σ_z^2) and $(\overline{D_y^2}, \overline{D_z^2})$, at this point we may consider the quantities $(\overline{Y^2}, \overline{Z^2})$ to be fully described by the expression equivalent to equation (14):

$$\left. \begin{aligned} \overline{Y^2}(x) &= \sigma_y^2(x) - \overline{D_y^2}(x) \\ \overline{Z^2}(x) &= \sigma_z^2(x) - \overline{D_z^2}(x) \end{aligned} \right\} \quad (65)$$

Instantaneous Plume Displacements, D_y and D_z

The displacement vector (D_y, D_z) of the instantaneous plume centerline displacement measured from the axis of the mean plume characterizes the stochastic

nature of the instantaneous plume. Gifford (1959) *assumed* that the frequency functions of D_y and D_z were *independent* and of *Gaussian form*. While both assumptions seem reasonable, at the time that Gifford made them there was virtually no observational data to either contradict or support this aspect of the model.

With the advent of lidars, Hamilton (1969) was able to make observations of the instantaneous properties of a power station plume at a distance of about two kilometers. At that distance, the *mean* instantaneous size of the plume was about 250 meters in the vertical and 400 meters in the horizontal. The scatter of the positions of the instantaneous centerline was similar in extent, with the crosswind scatter exceeding the vertical scatter. This is equivalent to the statements already employed in this section that on average, $\overline{Y^2}$ and $\overline{D_y^2}$ are each about $\frac{1}{2}\sigma_y^2$ and similarly $\overline{Z^2}$ and $\overline{D_z^2}$ are each about $\frac{1}{2}\sigma_z^2$. The frequency of incidence of the plume at various distances from the mean position of its center had a distribution in the horizontal close to Gaussian. In the vertical, the overall distribution was skewed, but the distribution below the mean position was also fairly close to Gaussian. The skewness above the mean positions was thought to be a result of more effective dispersion at the higher altitudes. Consequently, discounting effects of vertical anisotropies in the turbulent eddy transport which are beyond the scope of the current model, the Gaussian assumption appears to be well founded.

Beyond the above observations, a number of other requirements of a qualitative nature can be stated. If a single realization of the plume is viewed, as in a photograph, it has a sinuous appearance with both the amplitude and effective local wavelength of the sinuosities increasing with downwind distance from the source. Both appearances are due to the increasing scale with downwind distance of the class of eddies most effective in dispersing the plume (section II). From the point of view of modeling (D_y, D_z) , this suggests a quasi-sinusoidal form with the wavelength and amplitude proportional to the downwind distance x , or equivalently, proportional to each other. The amplitude of the stochastic vector (D_y, D_z) is specified in a time average sense by the standard deviations $(\sqrt{\overline{D_y^2}}, \sqrt{\overline{D_z^2}})$ which have already been discussed.

Certain statistical requirements may also be specified for (D_y, D_z) based on general physical arguments:

- (1) The time average at any fixed position x is zero, i.e. the expected value of the instantaneous plume centerline is just the centerline of the time-averaged plume, by definition.
- (2) The variances (time-average of the squares) of (D_y, D_z) are $(\overline{D_y^2}, \overline{D_z^2})$, by definition. Based on previous discussion, these variances increase with increasing downwind distance x , up to some limiting value.
- (3) For fixed x , the time autocorrelations approach zero with increasing time separation, due to the randomness and dissipative nature of the turbulent eddies.
- (4) The time average of the product of centerline displacements at two different positions at the same time approaches zero with increasing spatial separation, i.e. the spatial autocorrelations approach zero due to the randomness and dissipative nature of the turbulence.

A fifth requirement has been already noted, i.e.:

- (5) The probability distributions in time of D_y and D_z at any fixed position x are Gaussian.

The functional forms for (D_y, D_z) described below satisfies these criteria. To develop it required some effort which has been partially recapitulated in Appendix A.

In summary then, the displacement vector (D_y, D_z) is given by the relations:

$$\left. \begin{aligned} D_y(x,t) &= f_y(x) \gamma_{1_y}(t) \sin \left[\frac{2\pi}{c(f_y(x)+\epsilon)} \gamma_{2_y}(t)(x-\bar{U}t) \right] \\ D_z(x,t) &= f_z(x) \gamma_{1_z}(t) \sin \left[\frac{2\pi}{c(f_z(x)+\epsilon)} \gamma_{2_z}(t)(x-\bar{U}t) \right] \end{aligned} \right\}, \quad (66)$$

where ϵ is a small positive number, used to prevent singularity at the origin (in practice, ϵ is approximately equal to the inner diameter of the stack).

$$\left. \begin{aligned} f_y(x) &= \sqrt{\overline{D_y^2}(x)} \\ f_z(x) &= \sqrt{\overline{D_z^2}(x)} \end{aligned} \right\}, \quad (67)$$

$$\left. \begin{aligned} \gamma_{1_y}(t) &= \sqrt{u_{1_y}^2(t) + u_{2_y}^2(t)} \\ \gamma_{1_z}(t) &= \sqrt{u_{1_z}^2(t) + u_{2_z}^2(t)} \end{aligned} \right\}, \quad (68)$$

$$\left. \begin{aligned} \gamma_{2_y}(t) &= \sqrt{u_{3_y}^2(t) + u_{4_y}^2(t)} \\ \gamma_{2_z}(t) &= \sqrt{u_{3_z}^2(t) + u_{4_z}^2(t)} \end{aligned} \right\}, \quad (69)$$

where $(u_{1_y}, u_{1_z}, u_{2_y}, u_{2_z}, u_{3_y}, u_{3_z}, u_{4_y}, u_{4_z})$ are solutions to the differential equations:

$$\left. \begin{aligned} \dot{u}_{1_y}(t) &= -\frac{1}{T_y} u_{1_y} + v_{1_y} \\ \dot{u}_{1_z}(t) &= -\frac{1}{T_z} u_{1_z} + v_{1_z} \end{aligned} \right\}, \quad (70)$$

$$\left. \begin{aligned} \dot{u}_{2_y}(t) &= -\frac{1}{T_y} u_{2_y} + v_{2_y} \\ \dot{u}_{2_z}(t) &= -\frac{1}{T_z} u_{2_z} + v_{2_z} \end{aligned} \right\}, \quad (71)$$

$$\left. \begin{aligned} \dot{u}_{3y}(t) &= -\frac{1}{T_y} u_{3y} + v_{3y} \\ \dot{u}_{3z}(t) &= -\frac{1}{T_z} u_{3z} + v_{3z} \end{aligned} \right\} , \quad (72)$$

$$\left. \begin{aligned} \dot{u}_{4y}(t) &= -\frac{1}{T_y} u_{4y} + v_{4y} \\ \dot{u}_{4z}(t) &= -\frac{1}{T_z} u_{4z} + v_{4z} \end{aligned} \right\} , \quad (73)$$

The time constants are given by,

$$\left. \begin{aligned} T_y &= \frac{cf_y(\infty)}{\bar{U}} \\ T_z &= \frac{cf_z(\infty)}{\bar{U}} \end{aligned} \right\} , \quad (74)$$

The scaling constant between the local amplitude and effective wavelength is:

$$c \approx 6 \quad (75)$$

where, $(v_{1y}, v_{1z}, v_{2y}, v_{2z}, v_{3y}, v_{3z}, v_{4y}, v_{4z})$ are uncorrelated Gaussian processes (white noise components) with zero mean and variances given by

$$\left. \begin{aligned} Ev_{1y}(t)v_{1y}(t+\tau) &= Ev_{2y}(t)v_{2y}(t+\tau) = \frac{2}{T_y} \delta(\tau) \\ Ev_{3y}(t)v_{3y}(t+\tau) &= Ev_{4y}(t)v_{4y}(t+\tau) = \frac{8}{\pi^2 T_y} \delta(\tau) \end{aligned} \right\} \quad (76)$$

$$\left. \begin{aligned} Ev_{1z}(t)v_{1z}(t+\tau) &= Ev_{2z}(t)v_{2z}(t+\tau) = \frac{2}{T_z} \delta(\tau) \\ Ev_{3z}(t)v_{3z}(t+\tau) &= Ev_{4z}(t)v_{4z}(t+\tau) = \frac{8}{\pi^2 T_z} \delta(\tau) \end{aligned} \right\} \quad (77)$$

where $\delta(\tau)$ is the Dirac delta function.

The limiting amplitude is given by,

$$\left. \begin{aligned} f_y(\infty) &= \sqrt{\overline{D_{y\infty}^2}} \\ f_z(\infty) &= \sqrt{\overline{D_{z\infty}^2}} \text{ or } \sqrt{\overline{D_{zL}^2}} \text{ (when mixing height effects dominate)} \end{aligned} \right\} \quad (78)$$

$\overline{D_y^2}(x)$, $\overline{D_z^2}(x)$, $\overline{D_{y\infty}^2}$, $\overline{D_{z\infty}^2}$, and $\overline{D_{zL}^2}$ have been discussed previously in this section.

It then follows that $(\gamma_{1y}(t), \gamma_{1z}(t), \gamma_{2y}(t), \gamma_{2z}(t))$ have probability density functions:

$$\left. \begin{aligned} f_{\gamma_{1y}} &= y \exp\left[-\frac{y^2}{2}\right] \\ f_{\gamma_{1z}} &= z \exp\left[-\frac{z^2}{2}\right] \\ f_{\gamma_{2y}} &= \frac{y\pi^2}{4} \exp\left[-\frac{\pi^2 y^2}{8}\right] \\ f_{\gamma_{2z}} &= \frac{z\pi^2}{4} \exp\left[-\frac{\pi^2 z^2}{8}\right] \end{aligned} \right\} \quad (79)$$

It may be appropriate at this point to explore another model for the center-line dispersion. Two salient characteristics of the center-line dispersion are that it is normally distributed and correlated in time. If such characteristics were to be found in an ordinary (not partial) differential system, then the model would be taken as:

$$\dot{d} = -\lambda d + u, \quad \lambda > 0, \quad (80)$$

where u is Gaussian white noise with covariance:

$$Eu(t)u(t+\tau) = q\delta(\tau) , \quad (81)$$

giving

$$Ed(t)d(t+\tau) = q \frac{e^{-\lambda|\tau|}}{2\lambda} . \quad (82)$$

Now this is fine for $d(x_0, t)$ where x_0 is fixed. But how do we use this model to calculate $d(x, t)$ for all x and fixed time? If we use this as the amplitude of a sinusoid there are at least four problems: The amplitude and wave length must be multiplied by an increasing function of x ; when d passes through zero, the function is zero for all x ; the correlation doesn't go to zero with increasing x ; the distribution is not normal.

Moreover, there is a fundamental problem connected with the use of this type of model. In an error analysis it is necessary to have a noise-free nominal solution which contains all the structure needed in the analysis. In this model, the noise free solution is zero and thus the plume does not fluctuate. To avoid this problem a model such as (66) (with $\gamma_1(t)$ set to a constant value) would be required anyway. Consequently we have formulated the system (66)-(79) as a stochastic model with a deterministic model available merely by fixing $\gamma_1(t)$, $\gamma_{1_z}(t)$, $\gamma_{2_y}(t)$ and $\gamma_{2_z}(t)$ at typical values.

**Page
Intentionally
Left Blank**

V. SIMPLIFIED REMOTE AND IN SITU MEASUREMENTS MODELS

The initial concern will be with more or less idealized models representative of typical remote and *in situ* measurement types. The models will include the general characteristics of a broad class of measurement types and will avoid incorporating specifics that are peculiar to a particular measurement system. Within the scope of these generalized characteristics, the measurements will be assumed to provide a "perfect" quantification of the measured quality, except for random measurement noise of zero mean.

This will serve to:

- (a) Avoid additional complicating factors in the mathematical analysis that might obscure the initial research effort.
- (b) Avoid selecting a specific measurement system which is in fact under development or experimental at the present time and, consequently, subject to change.
- (c) Provide insight into the advantages to be gained in actual applications by the ultimate improvement of existing and prospective measurement systems.

The measurement models described in this section will be used in conjunction with the instantaneous and time-averaged pollutant dispersion models, parameter functional forms and *a priori* information described in Sections III and IV.

Remote Measurement Models

A number of instrument systems, at various stages of design and development, have been proposed for remote measurement of a variety of air pollutants. While a certain class of optical sensors with a high threshold of sensitivity can be employed to provide essentially *point* measurements of smoke stack emissions, many instruments and important applications involve so called long-path or open-path sensing which provides a spatial integral or average of some kind. Similarly, remote measurements can involve time averages, but many important aircraft and

satellite based techniques of interest here are more or less instantaneous. We will employ the term "remote" or "fast response remote" to imply instantaneous space-averaged measurements, unless specified as "slow response remote". Remote sensors are most often considered for application from airborne or space platforms. However, many of these techniques are applicable for ground based systems. As a basis for the remote measurement model, we will consider a downward (nadir) looking, non-imaging sensor based on a remote platform, which in practice will be either an aircraft or an earth orbiting satellite. The field of view of the instrument will then approximate a right circular cone (Figure 4.0) with the apex at the platform altitude, $z = z_p$. For current state of the art sensors, the plane half-angle field of view ϕ (Figure 4.0) is about 0.05 radians (Friedman and Ghovanlou, 1974). This corresponds to a "footprint" (circular base of the cone) diameter of about 100 km for a satellite at an altitude near 1000 km.

Proposed environmental monitoring satellite instruments are expected to have a footprint diameter in the range 40-100 km (Smith, Green and Young, 1974a). For a high flying aircraft (18-20 km) in the stratosphere well above the tropopause, sensors with the same field of view will provide a footprint diameter of about 2 km. The footprint would be reduced further for a low flying aircraft. For an aircraft flying near the tropopause at about 10 km the footprint for the same field of view would have about a 1 km diameter. It is reasonable to suppose that advances in the state-of-the-art will soon reduce the feasible footprint diameter to the 100 meter range for aircraft based instruments. In any case, further reductions by a factor of three or four in the sensors normal field of view can usually be achieved by application of external optics.

There are a number of *time constants* associated with actual sensors, which will be idealized in the present treatment. The instrument *lag time*, T_0 , is the time required to produce the first output response after exposure to an input signal (a step forcing function for definition purposes). It will be assumed that:

$$T_0 = 0$$

Some remote sensors can produce output data on a continuous basis. These "analog" devices include dispersive and non-dispersive correlation spectrometers, laser absorption spectrometers and radiometers (Friedman and Ghovanlou, 1974).

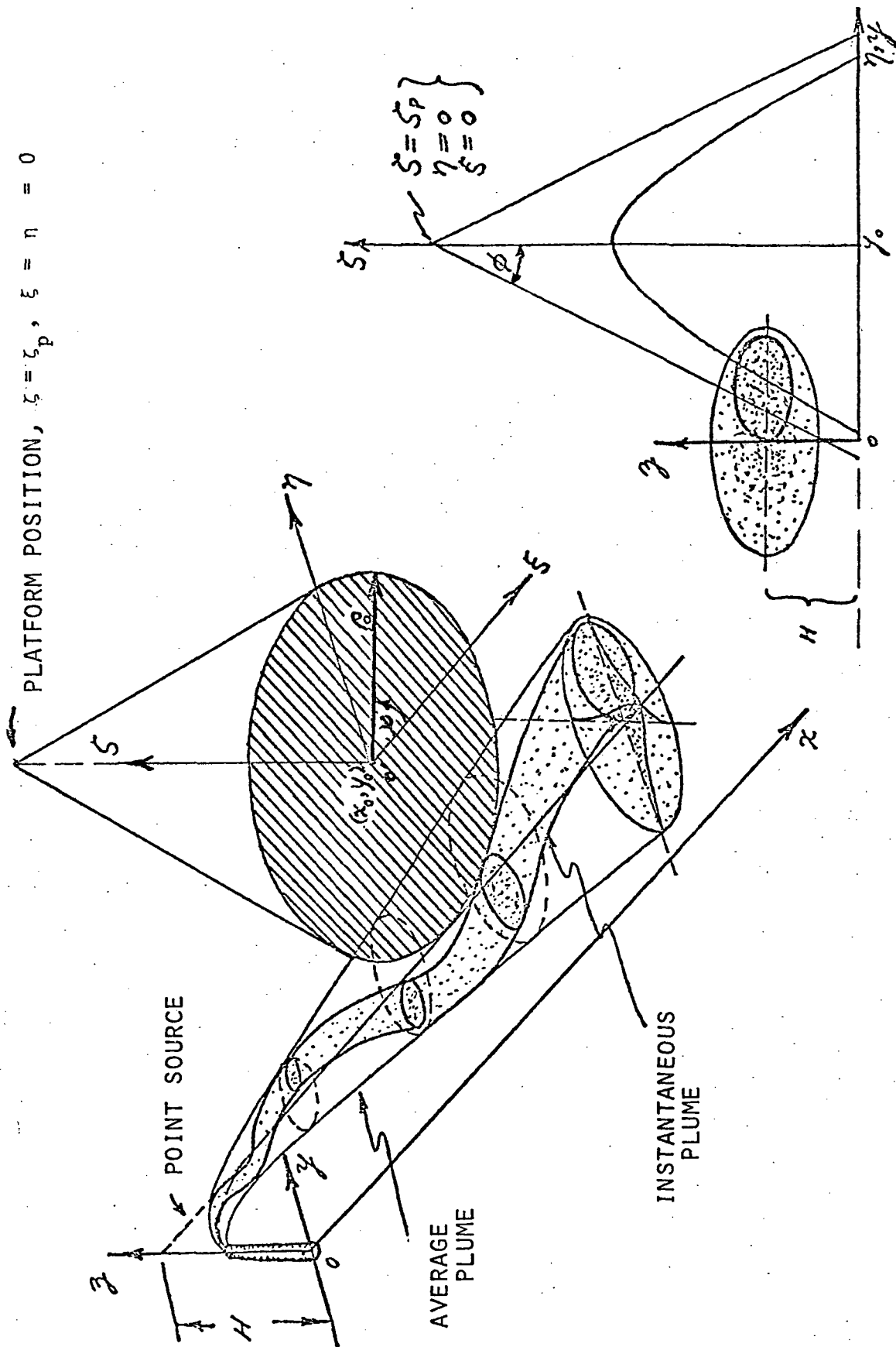


Figure 4.0 Geometry of Remote Sensor Field of View, Instantaneous Point Source Plume and Average Point Source Plume.

However, certain sensors require a finite *collection time*, T_C , to accumulate sufficient input data to produce a single satisfactory output datum. These sensors include interferometers of all kinds. In some cases, T_C may be the time required for a single scan taken at a slow rate with a long time constant. In other cases, T_C may consist of the total time of a series of scans of short time constant, i.e. $T_C = ST_S$, where S is the number of scans per datum and T_S is the time per scan. The series of scans is then averaged to produce the single output datum. In either case, we will assume that:

$$\frac{v_g T_C}{D_f} \ll 1, \quad (82)$$

where D_f is the diameter of the footprint and v_g is the ground-track speed of the platform.^{††}

Another time constant, associated with analog sensors, is the *response time* T_R , which is the time required for the amplitude of the output signal to reach $(1 - \frac{1}{e}) \approx 63\%$ of the peak value in response to step forcing function input. While in the field of view, the input element produces a response which has the time dependent form, $[1 - \exp(-t/T_R)]$. The response decays as $\exp(-t/T_R)$, when the input element leaves the field of view. We will assume that:

$$\frac{v_g T_R}{D_f} \ll 1. \quad (83)$$

On the basis of the above conditions, a single output datum of the sensor can be assumed to represent the total burden of the pollutant of interest contained within the conical field of view at that instant. However, the total burden will still be a time average over T_R or T_C (whichever is applicable) as far as the plume is concerned. However, if the instrument time constant (T_R or T_C) is small compared with the time scale of the plume fluctuations within the field of view, then the measurement can be assumed to be instantaneous, i.e. the measurement refers to the fluctuating plume.

The scale of eddies, ℓ , which are the dominant source of the plume fluctuations have a spatial range $D < \ell < L$ (Section II), where D is the average instantaneous plume width (crosswind for the current application) and L is the

^{††} For a high altitude spacecraft, the platform trajectory speed, v , may be substantially greater than the ground-track speed v_g . For an aircraft, $v \approx v_g$.

downwind distance from the source. As a measure of D we may take an average value of four standard deviations $\sqrt{Y^2}$ of the instantaneous plume crosswind material distribution at the downwind location of the instantaneous groundtrack position. The value of four standard deviations is based on two standard deviations on either side of the instantaneous centerline. On the average (Section IV), $Y^2 \sim \frac{1}{2}\sigma_y^2$, so that the average value of D is then $\approx 4E\left\{\sqrt{Y^2}\right\} \sim 2\sqrt{2}\sigma_y$. Using $x = L$ in equation (16), $D \approx 2\sqrt{2}\sigma_y^0 L^P$. Since the characteristic time scale of the fluctuations is $\delta\tau \sim \frac{\ell}{U}$ (Section II), we have $2\sqrt{2}\sigma_y^0 \frac{L^P}{U} < \delta\tau < \frac{L}{U}$. Consequently, the measurement may be assumed to apply to the fluctuating plume whenever:

$$(T_C; T_R) < 2\sqrt{2}\sigma_y^0 \frac{L^P}{U} \quad (84)$$

In practice, if more than one source is involved, the range of distances from the sources may be large. In that case, we may replace L in equation (84) by the minimum value L_{\min} that is of practical concern. L_{\min} must be defined by the horizontal resolution r_{Ih} of the measurements, so that:

$$(T_C; T_R) < 2\sqrt{2}\sigma_y^0 \frac{(r_{Ih})^P}{U} \quad (85)$$

for the fluctuating plume.

Similarly, the measurement may be rigorously applied to the average plume (i.e. the *expected value* of the fluctuating plume), whenever:

$$(T_C; T_R) > \frac{L}{U} \quad (86)$$

Actually, L is only an upper bound for D, so that the average plume will probably be a valid representation for averaging times somewhat shorter than L/\bar{U} . The averaging times, $\delta t \sim \frac{L}{\bar{U}}$, for the average plume based on a nominal wind speed of $\bar{U} = 5\text{m/sec}$ ($\sim 10\text{ miles/hr}$) are given in Section II. It should be noted that in terms of the (x,y,z) coordinate system, defined in Section III, $x \equiv L$.

If equation (82) is violated, the measurement model is no longer concerned with the volume of a cone but with the locus of the cone along a segment of the ground-track. If T_C is so large that condition (84) is violated, but not large enough to satisfy condition (86) for the spatial scales, L, of interest, then the measurement model is not strictly representative of *either* the fluctuating plume concentration *or* the limiting expected value of the fluctuating plume.

The rigorous concentration expression will then be the time average concentration:

$$\frac{1}{T_C} \int_0^{T_C} X(x,y,z,t;H) dt ,$$

where X is the instantaneous plume concentration. Consequently, the only class of remote measurements relevant to the current state of the art of sensor-platform configurations which allows the minimum of mathematical modeling complications is the category of *fast response remote* measurement satisfying conditions (82), (83) and (84).

With the above restrictions, the measurement may be modeled as (Smith, Young and Green, 1974b):

$$\bar{\Phi}(t) = K_0 \iiint_{V_C} J(z) X(x,y,z,t;H) dV + K_1 + \epsilon_0 \quad (87)$$

where V_C is the volume of the conical field of view, K_0 , is the instrument gain or sensitivity, K_1 is the instrument bias, ϵ_0 is the random error in the measurement with zero mean and variance σ_{obs}^2 and $J(z)$ is an altitude dependent weighting function. $X(x,y,z,t;H)$ is the instantaneous concentration of the plume (equation 12).

The weighting function $J(z)$ is a highly instrument dependent function. In keeping with our immediate objective of simplicity, we will assume that $J(z) \equiv 1$, $0 \leq z \leq \infty$. We will also assume that $K_0 = 1$ and $K_1 = 0$ in equation (87). In addition to the (x,y,z) Cartesian coordinate system used in equation (12) and described in Section III, a subsidiary Cartesian coordinate system (ξ, η, ζ) , convenient to the remote measurement geometry, will also be employed (Figure 4.0). The origin of the (ξ, η, ζ) system is at the subplatform point or instantaneous ground-track position given by $(x = x_0, y = y_0, z = 0)$. The platform is at $z = \zeta = \zeta_p$. The plane half-angle field of view is ϕ , as previously noted. The transformation is given by:

$$\left. \begin{aligned} \xi &= x - x_0 \\ \eta &= y - y_0 \\ \zeta &= z \end{aligned} \right\} \quad (88)$$

Then, equations (12) and (87) give:

$$\begin{aligned} \bar{\Phi}(t) &= \frac{Q}{2\pi U} \iint_{A_0} [\bar{Y}^2(\xi; x_0) \bar{Z}^2(\xi; x_0)]^{-1/2} \exp \left\{ \frac{-[\eta + y_0 - D_y(\xi, t; x_0)]^2}{2\bar{Y}^2(\xi; x_0)} \right\} \times \\ &\quad \left(\int_{\zeta=0}^{\zeta=\zeta_p - \rho \cot \phi} \exp \left[-\frac{[\zeta - H - D_z(\xi, t; x_0)]^2}{2\bar{Z}^2(\xi; x_0)} \right] \right. \\ &\quad \left. + \exp \left[-\frac{[\zeta + H + D_z(\xi, t; x_0)]^2}{2\bar{Z}^2(\xi; x_0)} \right] \right\} d\zeta \, dA \end{aligned} \quad (89)$$

where A_0 is the area of the circular base of the cone, $\rho^2 = \xi^2 + \eta^2$, and $\rho_0^2 = \zeta_p^2 \tan^2 \phi$.

The inner integral (over ζ) which we will denote by $\bar{\Phi}_\zeta$, has two parts. One part, corresponding to the point source, has $\zeta - H - D_z$ in the exponential and one part, corresponding to the image source, has $\zeta + H + D_z$ in the exponential. We will denote these two parts of the inner integral as $\bar{\Phi}_{\zeta-}$ and $\bar{\Phi}_{\zeta+}$, respectively, so that $\bar{\Phi}_\zeta \equiv \bar{\Phi}_{\zeta+} + \bar{\Phi}_{\zeta-}$. $\bar{\Phi}_{\zeta\pm}$ can be expressed in terms of error functions (Abramowitz and Stegun, 1970), so then:

$$\begin{aligned} \bar{\Phi}_\zeta &= \sqrt{\frac{\pi \bar{Z}^2}{2}} \left\{ \operatorname{erf} \left[\left(\frac{1}{2\bar{Z}^2} \right)^{-\frac{1}{2}} (\zeta_p - \rho \cot \phi + H + D_z) \right] \right. \\ &\quad \left. + \operatorname{erf} \left[\left(\frac{1}{2\bar{Z}^2} \right)^{-\frac{1}{2}} (\zeta_p - \rho \cot \phi - H - D_z) \right] \right\} \end{aligned} \quad (90)$$

The complete integral, equation (87) can be expressed in terms of (ξ, η) or, equivalently, in terms of the polar coordinates (ρ, ψ) as shown in Figure 4.0. The expression in terms of (ξ, η) has an advantage in that none of the dispersion parameters D_y, D_z, Y^2, Z^2 depend upon η . However, the complicated manner in which η enters the argument of the error functions in the integrand does not lend itself to the application of standard incomplete integral expressions in terms of special functions, so that in either case the area integral must be done numerically.

Smith, Green and Young (1974a) have presented a technique for the numerical integration of equations (89) and (90) in modified polar coordinates. They point out that the cartesian coordinate system (ξ, η) requires a very fine rectangle grid to obtain a reasonably good fit to the circular boundary, whereas the conventional polar coordinate system tends to concentrate in the region of the origin the points at which the function is evaluated, and leave these points relatively sparse in the outer portion of the region, when equal increments in $\Delta\psi$ are employed.

Equations (89) and (90) can be simplified considerably for the special situation where the platform is a satellite at very high altitude above the tropopause (altitude h_T), i.e. $\frac{h_T}{\zeta_p} \ll 1$, and the field of view is very narrow, $\tan \phi = \frac{\rho_0}{\zeta_p} \ll 1$. In that case, the conical field is approximated by a cylinder with the same footprint. An additional condition for the cylinder to be a good approximation of the cone below the tropopause is $\frac{h_T \tan \phi}{D_F} \ll 1$. The boundaries of the cylinder depart increasingly from the cone as $\zeta \rightarrow \zeta_p$. However, at high platform altitudes, the integrand, X , will be vanishingly small since the plume concentration diminishes as a Gaussian away from the plume axis and most of the pollutants are effectively confined in the troposphere, in any case. Consequently, the integral can just as well be performed over the infinite cylinder ($\zeta_p \rightarrow \infty$) for this approximation. Then

$$\bar{\Phi}_{\zeta_\infty} = \int_0^\infty \left\{ \exp \left[-\frac{[\zeta-H]^2}{2Z^2} \right] + \exp \left[-\frac{[\zeta+H]^2}{2Z^2} \right] \right\} d\zeta = \sqrt{2\pi Z^2} \quad (91)$$

Then,

$$\bar{\phi}_{\infty}(t) = \frac{Q}{\sqrt{2\pi U}} \int_{\xi=-\rho_0}^{\xi=+\rho_0} \left[Y^2(\xi; x_0) \right]^{-\frac{1}{2}} \int_{\eta=-\sqrt{\rho_0^2-\xi^2}}^{\eta=+\sqrt{\rho_0^2-\xi^2}} \exp \left\{ - \frac{[\eta^2 + 2\eta(y_0 - D_y(\xi, t; x_0)) + (y_0 - D_y(\xi, t; y_0))^2]}{2Y^2(\xi; x_0)} \right\} d\eta d\xi \quad (92)$$

which can be integrated with respect to η (Abramowitz and Stegun, 1970):

$$\begin{aligned} \phi_{\eta\infty}(\xi, t, x_0, y_0) = & \sqrt{\frac{\pi Y^2}{2}} \left\{ \operatorname{erf} \left(\frac{1}{\sqrt{2Y^2}} \left[\sqrt{\rho_0^2 - \xi^2} + (y_0 - D_y) \right] \right) \right. \\ & \left. + \operatorname{erf} \left(\frac{1}{\sqrt{2Y^2}} \left[\sqrt{\rho_0^2 - \xi^2} - (y_0 - D_y) \right] \right) \right\} \end{aligned} \quad (93)$$

and

$$\bar{\phi}_{\infty}(t) = \frac{Q}{\sqrt{2\pi U}} \int_{\xi=-\rho_0}^{\xi=+\rho_0} \frac{\phi_{\eta\infty}(\xi, t; x_0, y_0)}{\sqrt{Y^2(\xi; x_0)}} d\xi \quad (94)$$

Integral (94) can be calculated using any number of standard numerical integration procedures, such as Simpson's Rule.

In spite of the convenience of the cylinder approximation, caution must be exercised before applying it, even when all the stated conditions are satisfied. A single remote measurement has very little inherent *vertical* resolution when considered in isolation. However, when the fields of view of a sequence of measurements *overlap*, then the regions of the intersections have a *potential* for providing much more vertical resolving power than any measurement of the sequence

has in isolation. If \dot{M} is the data rate (measurement/sec) then the condition for the intersection of successive footprints is $\frac{v \dot{M}}{D_f} < 1$.

In Situ Measurement Models

In situ measurement systems which depend on atmospheric sampling or direct physical contact of some kind are usually thought of in terms of ground based monitoring. However, some efforts are underway to apply certain *in situ* techniques to low altitude airborne platforms including helicopters. A distinction is sometimes made if a sample is taken *in situ* but analyzed some distance away and perhaps at a much later time as is often done with grab samples. In the transfer process, the sample may undergo changes so that it no longer provides a strict *in situ* measurement. Consequently, measurements of this type are sometimes referred to as "sample" measurements rather than "*in situ*" measurements. We will use the term "*in situ*" in a general sense to apply to measurements relevant to a particular point in space, although perhaps averaged over time in some way.

The *in situ* measurements of interest here can be categorized as being either instantaneous or time averaged, airborne or ground based, fixed site or mobile. We will confine our attention to *in situ* measurement which are relevant to a particular point in space. This specifically excludes the category of time averaged measurements taken from fast moving mobile platforms such as aircraft, even though these measurements involve atmospheric sampling or direct physical contact methods that usually define an *in situ* measurement. As a result, we will be concerned with:

- (A) a set of instantaneous point measurements relevant to the fluctuating plume concentration $X(x,y,z,t;H)$ (equation (12)):

$$\psi_{ij}(\vec{r}_i, t_j) = \left\{ K_i^0 X(\vec{r}_i, t_j) + K_i^1 + \epsilon_i^0 \right\} \quad (95)$$

$$i=1, \dots, n; j=1, \dots, m$$

where $\vec{r}_i \equiv (x_i, y_i, z_i)$. K_i^0 and K_i^1 are the gains and biases associated with the instruments at positions \vec{r}_i . ϵ_i^0 are the random errors in the measurements at position \vec{r}_i with zero mean and variances $(\sigma_i^0)^2$. We will assume that $K_i^0 = 1$ and $K_i^1 = 0$, for the current application. If the instantaneous measurements are taken continuously in time, then we are concerned with:

$$\psi_i(\vec{r}_i, t) = \{X(\vec{r}_i, t) + \epsilon_i^0\}, \quad i=1, \dots, n; \quad t_1 \leq t \leq t_2 \quad (96)$$

(B) a set of time averaged point measurements relevant to the average plume concentration $\bar{X}(x, y, z; H)$ (equation (1)):

$$\bar{\psi}_i(\vec{r}_i) = \{k_i^0 \bar{X}(\vec{r}_i) + k_i^1 + \bar{\epsilon}_i\}, \quad i=1, \dots, n \quad (97)$$

where k_i^0 and k_i^1 are the gains and biases associated with the instruments at position \vec{r}_i . $\bar{\epsilon}_i$ are assumed to be random errors of zero mean and variances σ_i^2 . Again, $k_i^0 = 1$ and $k_i^1 = 0$, in order to avoid instrument specifics. In practice there may be a set of measurements for each position \vec{r}_i taken at several times, t_j ($j=1, \dots, m$):

$$(\bar{\psi}_i)_{t_j} = (k_i^0 \bar{X}(\vec{r}_i) + k_i^1 + \epsilon_i)_{t_j}, \quad i=1, \dots, n; j=1, \dots, m \quad (98)$$

$\bar{X}(\vec{r}_i)$ has no time dependence over the time scale t_{met} during which the average values of the meteorological parameters (mean wind \bar{U} , mean wind direction θ , mixing height L , stability class, etc.) apply. In practice, the $(\bar{\psi}_i)_{t_j}$ which fall within the period $t_0 \leq t \leq t_0 + \Delta t$, $\Delta t \leq t_{met}$, are averaged to produce the $\bar{\bar{\psi}}_i$. If $(\epsilon_i)_{t_j}$ are also assumed to be random errors of zero mean and variances $(\sigma_i^2)_{t_j}$ and if the measurement times t_j are far enough apart to avoid serial correlations due to specific instrument time constants (i.e. no time correlations), then σ_i^2 (the variance of the average) is given by:

$$\sigma_i^2 = \frac{1}{m} \sum_{j=1}^m (\sigma_i^2)_{t_j}, \quad (99)$$

where

$$\bar{\Psi}_i = \frac{1}{m} \sum_{j=1}^m (\bar{\Psi}_i)_{t_j} \quad (100)$$

Otherwise, the calculation of $\bar{\sigma}_i^2$ must take into account the correlations resulting from the instrument specifics.

Considerations of Averaging Times

At this point it becomes necessary to become more precise in our use of the term "averaging time." One "averaging time" is a result of the finite response time of the instrument, consisting of the time constants of the electronics, the chemical processing times and inertia related to moving mechanical parts. Any high frequency fluctuations of the measured phenomenon that are more rapid than this time period are naturally filtered out and the information is irretrievably lost. We have employed the term "averaging time" or "instrument averaging time" for this time period, in conformance with convention in most of the literature.

Another kind of averaging time is a result of the finite period over which measurements are made. If the measurements are sampled and analytically averaged to produce a smoothed or average value, then the term "sampling time" or occasionally "measuring interval" is applied to this longer time period defined by the analytical processing. We have employed the term "averaging time" to mean either strict instrument "averaging time" or "sampling time", if the latter is applicable, for general discussion which is not specific to particular measurement types or processing procedures.

In equation (98), the time averages of the $(\bar{\Psi}_i)_{t_j}$ pertain to the instrument *averaging time*, whereas the time averages of the $\bar{\Psi}_i$ of equation (97) pertain to the *sampling time* Δt , if the $\bar{\Psi}_i$ were obtained from the $(\bar{\Psi}_i)_{t_j}$.

In the interest of simplicity, we are excluding the category of time-averaged *in situ* measurements taken from a rapidly moving platform. The model for this class of instruments involves calculation of a formal time average and path integral over a segment of the platform trajectory of the fluctuating plume concentration $X(\vec{r}, t)$.

In dealing with time averaged measurements, we will restrict our attention to averaging times ≤ 5 hours. This limit has been selected to approximate the time scale T which allows the direction of the mean wind θ to coincide to a reasonable degree with the observed direction of the actual wind at any random time point in an interval T (i.e. small variance). Experience suggests that the application of a mean wind (magnitude \bar{U} and direction θ) is quite good over an interval of 2-3 hours, but breaks down quite rapidly after 5 hours (Slade, 1968). The value of 5 hours also coincides with the appropriate averaging times for which the average plume model (i.e. the expected value of the fluctuating plume) will be valid at down wind distances ~ 100 km. The value of 100 km is also the characteristic dimension of a typical urban air quality control region.

If averaging times exceeding 5 hours were to be considered, then higher order statistics than the mean value would have to be taken into account for the prevailing wind, mixing height, stability class, etc. The model then involves a variable wind direction, and other variable meteorological parameters which are *stochastic variables* governed by probability distributions. A treatment of this problem has been given by Calder (1970) for application with the standard Gaussian (i.e. average value) elevated point source plume model.

As previously noted (in Section II) for a given downwind position L from a point source, there is an averaging time (actually, time range) $\delta t \sim \frac{L}{\bar{U}}$ that will be just appropriate for the measurement to apply to the average plume representation (i.e. expected value fluctuating plume). This order δt is the value required to view approximately the same values of the state (e.g. peak concentration) more than once, i.e. in order to properly average out the meandering effect. The average plume model still applies for averaging times δT much larger than this (i.e. $\delta T \gg \delta t$), assuming that the average wind is still a valid concept. However, the representation then includes the dispersion effects of the larger scale eddies that an observer at position L would attribute to fluctuations in the mean wind (Scorer, 1968). The average plume is then broader (i.e. larger values of σ_y and

and σ_z) and exhibits a smaller peak value at position L. If $\delta T \ll \delta t$, then the correct local representation is given by the fluctuating plume.

In the current application, we will be mixing *a priori* data with various measurement types having different fundamental time scales. These measurements will generally be made at different positions over an urban area, and will pertain to various scattered sources. If consistency is to be achieved in the estimation procedure, then a technique for relating *all* these divergent time and space scales of the measurements and the phenomenon will be required.

The *a priori* values of $\sigma_y(x)$ and $\sigma_z(x)$ are based on the curves given by Turner (1970). These curves and the corresponding functional representations have been discussed in Section IV. The applicable wind speeds range from $\bar{U} < 2\text{m/sec}$ to $\bar{U} > 6\text{m/sec}$, depending on stability conditions (Turner, 1970). Turner (1970) reports that these curves "are representative for a sampling time of about 10 minutes". However, this must apply to the smaller distances, since $\delta t \sim L/\bar{U}$ implies that for any reasonable wind speed, a sampling time of 10 minutes at the 100 km downwind distance would still apply to the fluctuating plume! Most of the original data was in fact taken at distances $< 1\text{ km}$ from the source and with very little data near 100 km, so that the curves are essentially extrapolations at the greater distances (Pasquill, 1974). Turner has indicated reasonable accuracy for distances ranging from "a few hundred meters to 10 km or more" depending on stability conditions. For a sampling time of ~ 10 minutes and wind speeds ranging from 1-10 meters/sec, $\delta t \sim L/\bar{U}$ implies values of L ranging from 600 meters to 6 km. Therefore, the *a priori* information based on Turner's curves can be taken to represent the shortest averaging time applicable to the average plume, which can then be approximated by $\delta t \sim L/\bar{U}$ for any downwind distance L.

Consider a measurement of given averaging time δT , positioned some arbitrary distance L downwind from the source. In terms of the (x,y,z) coordinate system of Section III, $L \equiv x$. In the following development, we will employ x, with the understanding that $x \equiv L$ applies to the position of the measurement. This will serve the purposes of most estimation theory applications. However, for certain simulation purposes, one may be concerned with relating other positions x to the particular $x \equiv L$ in a specific way. This problem will be considered following the main development.

As previously noted, at position $x \equiv L$ the characteristic time scale $\delta \tau$ of the

eddies governing the crosswind fluctuations is given by the relation:

$$2\sqrt{2} \sigma_y^0 \frac{x^p}{U} < \delta\tau < \frac{x}{U} \quad (101)$$

where $\sigma_y^0 x^p$ is the *a priori* value determined from Turner (1970). Since the range of $\delta\tau$ is not precisely defined in any event, we will assume that equation (101) also defines the time scale for the vertical fluctuations. The condition for the measurement to strictly apply to the fluctuating plume is then $\delta T \leq 2\sqrt{2} \sigma_y^0 \frac{x^p}{U}$. For the measurement to strictly apply to the average plume model, the condition is $\delta T \geq \frac{x}{U}$. For δT within the range of $\delta\tau$ (equation (101)), then the actual time average of the fluctuating plume model is involved:

$$\langle X \rangle_{\delta T} = \frac{1}{\delta T} \int_{t_1}^{t_1 + \delta T} X(x, y, z, t; H) dt, \quad \delta T \sim \delta\tau \quad (102)$$

However, we will apply the measurement to the fluctuating plume model whenever δT is less than the midpoint of the range $\delta\tau$. Whenever δT is greater than or equal to the midpoint of the range of $\delta\tau$ then the measurement will be applied to the average plume model. Therefore, we define

$$\overline{\delta\tau} = \frac{x}{2U} (1 + 2\sqrt{2} \sigma_y^0 x^{p-1}) \quad (103)$$

so that the measurement applies to:

- (A) the fluctuating plume, i.e. the measurement is of the class $\overline{\Psi}_{ij}(\vec{r}_i, t_j)$, whenever $\delta T < \overline{\delta\tau}$;
- (B) the average plume, i.e. the measurement is of the class $\overline{\Psi}_i(\vec{r}_i)$, whenever $\delta T \geq \overline{\delta\tau}$. Considering the situation given by $\delta T \geq \overline{\delta\tau}$ further:
 - (a) when $\overline{\delta\tau} \leq \delta T \leq \frac{x}{U}$ then, we will assume that the measurement applies to the plume where the averaging time is *just* sufficient to average out the meandering effects of the dominant class of eddies. We have previously denoted the concentration for this plume by \overline{X} with the plume variances $\sigma_y(x)$ and $\sigma_z(x)$. We will refer to \overline{X} as the *optimum* time averaged plume concentration.
 - (b) For the case $\delta T > \frac{x}{U}$, then the average plume applies with standard deviations $\overline{\sigma}_y(x, \delta T) > \sigma_y(x)$; $\overline{\sigma}_z(x, \delta T) > \sigma_z(x)$, and the average plume is broader and has a correspondingly smaller peak value (on the plume axis) than the optimum time-averaged plume for the same downwind position. We will denote the concentration expression for this plume by $\overline{\overline{X}}$.

The question now arises as to how to properly relate $\overline{\sigma_y}(x, \delta T)$ to $\sigma_y(x)$ and $\overline{\sigma_z}(x, \delta T)$ to $\sigma_z(x)$. The averaging time, corresponding to $\sigma_y(x)$ and $\sigma_z(x)$ is assumed equal to $\delta t \sim x/\bar{U}$. Turner (1970) citing the research of a number of investigators suggests the relationship for the concentration relevant to averaging times $\delta T > \delta t$:

$$\overline{\overline{X}} = \overline{X} \left(\frac{\delta t}{\delta T} \right)^s, \quad (104)$$

where $0.17 \leq s \leq 0.20$, and the relation is most appropriate for $\delta T < 2$ hours. $\overline{\overline{X}}$ and \overline{X} are the concentrations for averaging times δT and δt , respectively. Conservation of mass suggests a relation between the product of the peak values of average plume concentrations, Peak $(\overline{\overline{X}})$ and Peak (\overline{X}) , and the corresponding standard deviations of the plume material distributions $(\overline{\sigma_y}, \overline{\sigma_z})$ and (σ_y, σ_z) for all averaging times:

$$\begin{aligned} (\text{Peak } \overline{\overline{X}}) \cdot \overline{\sigma_y}(x, \delta T) \cdot \overline{\sigma_z}(x, \delta T) = \\ (\text{Peak } \overline{X}) \cdot \sigma_y(x) \cdot \sigma_z(x) \end{aligned} \quad (105)$$

The peak values Peak $(\overline{\overline{X}})$ and Peak (\overline{X}) occur on the plume axis, so that Peak $(\overline{\overline{X}}) = \overline{\overline{X}}(x, 0, H; H)$ and Peak $(\overline{X}) = \overline{X}(x, 0, H; H)$, where \overline{X} is given by equation (1) with $\sigma_y(x)$ and $\sigma_z(x)$ as the standard deviations, and $\overline{\overline{X}}$ is also given by equation (1) but with $\overline{\sigma_y}(x, \delta T)$ and $\overline{\sigma_z}(x, \delta T)$ as the standard deviations. Equations (104) and (105) give:

$$\overline{\sigma_y} \overline{\sigma_z} = \sigma_y \sigma_z \left(\frac{\delta T}{\delta t} \right)^s \quad (106)$$

Assuming the same dependence on averaging time for both $\overline{\sigma_y}$ and $\overline{\sigma_z}$, gives:

$$\frac{\overline{\sigma_y}}{\sigma_y} = \frac{\overline{\sigma_z}}{\sigma_z} = \left(\frac{\delta T}{\delta t} \right)^{\frac{s}{2}} \quad (107)$$

or in terms of the variances:

$$\frac{\overline{\sigma_y}^2}{\sigma_y^2} = \frac{\overline{\sigma_z}^2}{\sigma_z^2} = \left(\frac{\delta T}{\delta t} \right)^s \quad (108)$$

Williamson (1973) suggests that the peak concentration of the average plume will diminish as $\delta T^{-\frac{1}{2}}$ for values of δT between 10 minutes and 5 hours, while a $\delta T^{-1/5}$ dependence for the peak concentration seems appropriate for values of δT

less than 10 minutes. This again implies the validity of equation (108), but with $s = 1/2$, $10 \text{ minutes} < \delta T < 5 \text{ hours}$ and $s = 1/5$, $\delta T < 10 \text{ minutes}$. The value $s = 1/2$ agrees with some theoretical values based on statistical turbulence theories (Hino, 1968). For the dependence of crosswind standard deviation of the mean wind direction σ_θ on averaging time, Slade (1968) suggests:

$$\sigma_\theta(\delta T_1) = \left(\frac{\delta T_1}{\delta T_2} \right)^a \sigma_\theta(\delta T_2) \quad (109)$$

where $a \approx 1/5$ and since $\sigma_y \approx \sigma_\theta x$ equation (109) implies (108), but with $s \approx 2/5$. We will employ the relation:

$$\sigma_y^{-2}(x, \delta T) = \sigma_y^2 \left(\frac{\overline{U} \delta T}{x} \right)^s s(\delta T) \quad (110)$$

where the expected range of s is $0.15 \leq s(\delta T) \leq 0.50$, and *a priori* value is $s(\delta T) \approx 0.29$. The assumed functional form of $s(\delta T)$ is

$$s(\delta T) = \begin{cases} s_0, & \delta T < 10 \text{ minutes} \\ s_\infty, & \delta T \geq 10 \text{ minutes} \end{cases} \quad (111)$$

$s(\delta T)$ is now another function to be estimated, but can be assumed to be a function only of meteorological conditions, general topography, etc. so that it is *not a source dependent quantity*.

For the vertical variance σ_z^{-2} we will employ the relation parallel to equation (110), with σ_z given by equation (19):

$$\sigma_z^{-2}(x, \delta T) = \sigma_z^2 \left(\frac{\overline{U} \delta T}{x} \right)^s s(\delta T) \quad (112)$$

when there is no appreciable influence from a mixing ceiling.

The representation of $\sigma_z(x)$ for the situation where the influence of a mixing layer of altitude L will be felt has been given in Section IV (Equations (37)-(44)). In this representation, $\sigma_z(x)$ approaches a limiting value $\sigma_z(\infty) = \sigma_u(L, H) \approx \sigma_u(L, 0)$. Under no circumstances will an observer

employing an instrument with an averaging time δT , view the plume as having any appreciable penetration above the mixing ceiling, assuming that $H < L$. Therefore, $\overline{\sigma_z}(x, \delta T) \leq \sigma_u(L, H)$, for all δT and all x .

Following a concept similar to a proposal of Pasquill (1974) for representing the influence of the "lid" at altitude L , we will assume that there is virtually no influence on $\overline{\sigma_z}$ until it achieves a value $\frac{\sigma_u}{2}$. Therefore, we let $\overline{\sigma_z}$ be approximately described by the relation (given by the square root of equation (112))

$$\overline{\sigma_z}(x, \delta T) = \sigma_z \left(\frac{\overline{U} \delta T}{x} \right) \frac{s(\delta T)}{2} \quad (113)$$

up to point where $\overline{\sigma_z}$ is $\frac{\sigma_u(L, 0)}{2}$. In the region where equation (113) yields values of $\overline{\sigma_z} > \sigma_u$, we impose the condition $\overline{\sigma_z}(x, \delta T) \leq \sigma_u(L, 0)$ as a *weak* upper bound on $\overline{\sigma_z}$ in the sense that $|\sigma_u - \overline{\sigma_z}(x, \delta T)| < \epsilon \sigma_u$, $\epsilon \ll 1$, for all x and δT . In the region where equation (113) provides values of $\overline{\sigma_z}$ in the range $\sigma_u/2 < \overline{\sigma_z} \leq \sigma_u$, we require some smooth transition to the weak upper bound. A representation of the variance $\overline{\sigma_z}^2$, satisfying all of these conditions is:

$$\overline{\sigma_z}^2(x, \delta T) = \left\{ \overline{\sigma_z}^* K(\overline{\sigma_z}^*) + \sigma_u(L, 0) [1 - K(\overline{\sigma_z}^*)] \right\}^2 \quad (114)$$

$$\overline{\sigma_z}^*(x, \delta T) = \sigma_z(x) \left(\frac{\overline{U} \delta T}{x} \right) \frac{s(\delta T)}{2} \quad (115)$$

$$\sigma_u(L, 0) = \frac{L}{\sqrt{3}}, \text{ unless noted otherwise} \quad (116)$$

$$K(\overline{\sigma_z}^*) = \frac{1}{2} \left\{ 1 - \tanh \left[\frac{8\overline{\sigma_z}^* - 6\sigma_u}{\sigma_u} \right] \right\} \quad (117)$$

where $\sigma_z(x)$ is the representation for the vertical standard deviation or thickness parameter of the optimum time-averaged plume in the presence of a mixing layer (Eqns. (37) - (44)).

The properties of the function $K(\overline{\sigma_z}^*)$ are shown in Figure 5.0. The parameter $s(\delta T)$ in equation (115) is still given by equation (111). If, for estimation pur-

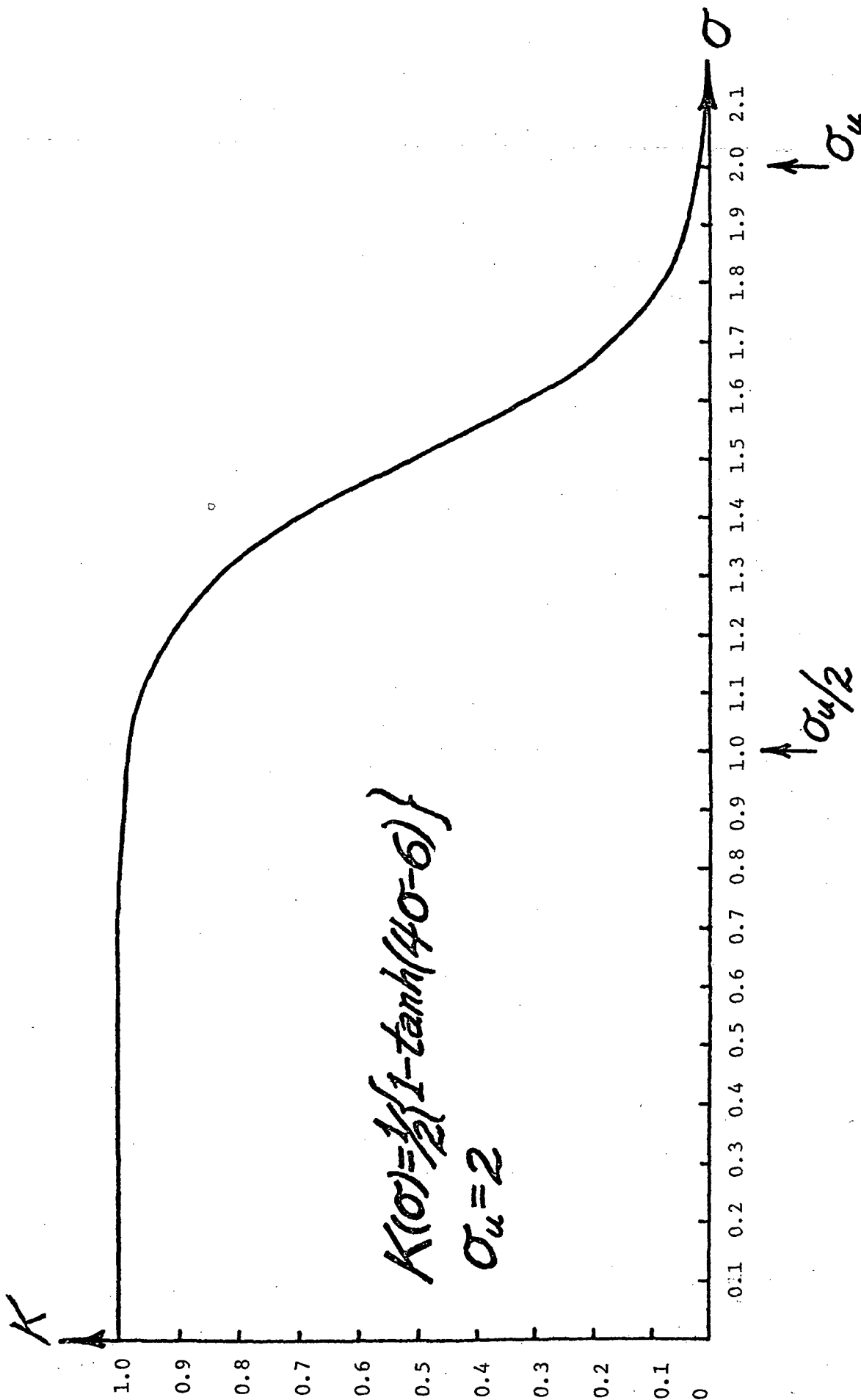


Figure 5.0 Properties Of The "Clipping" Function, $K(\sigma)$

poses, a smooth transition is desirable between s_0 and s_∞ in $s(\delta T)$, rather than a step discontinuity at $\delta T = 10$ minutes, this can be provided. Referring to the data presented graphically by Hino (1968), the transition probably takes place smoothly in the range $9 \text{ minutes} \leq \delta T \leq 12 \text{ minutes}$.

If we let δT_L equal the lower bound of the transition range, i.e. $\delta T_L \approx 9$ minutes, and δT_u equal the upper bound of the transition range, i.e. $\delta T_u \approx 12$ minutes, then an appropriate interpolation function can be formulated by analogy with the function $I(x)$ formulated for application with $\sigma_z^2(x)$ and $D_z^2(x)$ (Section IV):

$$\left. \begin{aligned} I_t(\delta T) &= \frac{1}{2} \left(1 + \tanh \frac{2(\delta T - \bar{\delta T})}{\delta T_u - \delta T_L} \right) \\ \bar{\delta T} &= \frac{\delta T_u + \delta T_L}{2} \end{aligned} \right\} \quad (118)$$

Then,

$$s(\delta T) = s_0(1 - I_t(\delta T)) + s_\infty I_t(\delta T) \quad (119)$$

If, for any reason it is of interest to *simulate* the plume corresponding to the measured plume at downwind position x (with an instrument having an averaging time δT) at any other downwind position x_1 , then \bar{X} is given by equation (1) with $\bar{\sigma}_y$ and $\bar{\sigma}_z$ given by:

$$\left. \begin{aligned} \bar{\sigma}_y(x_1, \delta T) &= \sigma_y(x_1) \left(\frac{\bar{U} \delta T}{x} \right) \frac{s(\delta T)}{2} \\ \bar{\sigma}_z(x_1, \delta T) \text{ (or } \bar{\sigma}_z^*(x_1, \delta T) \text{ in the presence} \\ &\text{of a mixing layer)} \\ &= \sigma_z(x_1) \left(\frac{\bar{U} \delta T}{x} \right) \frac{s(\delta T)}{2} \end{aligned} \right\} \quad (120)$$

If, however, one wanted to *measure* the plume corresponding to the measured plume at downwind position x (with an instrument having an averaging time δT) at any other downwind position x_1 , then a different instrument averaging time δT_1 is required:

$$\delta T_1 = \frac{x_1 \delta T}{x} \quad (121)$$

It should also be noted, that while an estimator will adjust certain parametric constants it cannot alter the basic physical assumptions of the model. For example, the variance of the crosswind plume dispersion of the steady-state plume has been *assumed* to follow a power law relation:

$$\sigma_y^2 = (\sigma_y^0)^2 x^{2p} .$$

The estimator cannot change this assumption! What it can do, however, is adjust the values of the constants σ_y^0 and p . With the addition of an estimation algorithm to the air quality simulation model, certain physical parameters such as σ_y^0 and p are no longer *fixed* aspects of the simulation but are automatically adjusted to provide the best approximation of reality implicit in the measurements. These measurements also have associated uncertainties which the estimator takes into account.

The measurement models developed in this section, in turn, employ the dispersion models for the instantaneous and time averaged concentrations (X and \bar{X}) presented in Section III and the individual parameter models and *a priori* information developed in Section IV. This completes the basic mathematical modeling required for the application of formal estimation theory techniques to the problem of air quality estimation for elevated point sources.

**Page
Intentionally
Left Blank**

VI. CONCLUSIONS

The application of estimation theory, which originated in guidance and control research, to the analysis, interpretation and use of the various types of air quality measurements in conjunction with pollutant dispersion simulation models can provide a cost-effective method of obtaining reliable area-wide air quality estimates. In order to apply estimation theory, one requires not only parameterized dispersion models but measurement models consistent with the measurement processes of interest, as well. These two areas of modeling involved in the estimation process must be mutually consistent in terms of their fundamental assumptions and approximations. The same internal consistency is required for the incorporation of any *a priori* information concerning the physical processes and model parameters. The application of *a priori* parameters alone with diffusion models corresponds to conventional simulation practice. The optimum combination of *a priori* knowledge (plume parameters and uncertainties) and air quality measurements in conjunction with plume models through a systematic parameter estimation procedure to provide improved air pollutant dispersion simulations is the ultimate objective of the current research effort.

One of the principal features of the model development described in the previous sections is a method for low dimensional modeling (in terms of the estimation state vector) of the instantaneous and time-averaged pollution distribution. In summary, some of the specific aspects of the results discussed in the preceding sections are:

a) Extension of the fluctuating plume model of Gifford (1959) to provide an expression for the instantaneous concentration X due to an elevated point source. This model has the important property that the formal calculation of its statistical expected value is identified with the expression for the mean plume concentration \bar{X} based on the Gaussian point source plume model given by Turner (1970). Formal mathematical relationships between the basic parameters of the fluctuating and steady-state plume models then provide a theoretical basis for relating instantaneous and time-averaged plume measurements.

b) Development of individual models for each of the parameters appearing in both the instantaneous and time-averaged plume equations, including the stochastic properties of the instantaneous fluctuating plume. The particular requirements of the estimation theory application have been factored into the model development.

c) Development of models of the various measurement types for application with real measurement data and the plume models in an estimation procedure.

The various levels of model development provide a basis for the systematic incorporation of *a priori* dispersion knowledge and associated uncertainties with different measurement types using estimation theory techniques to provide air quality estimates on self-consistent time scales.

VII. REFERENCES

1. Abramowitz, M. and Stegun, I.A.: Handbook of Mathematical Functions with Formulas, Graphs and Mathematical Tables, National Bureau of Standards, Applied Math Series 55, Issued June 1964, corrected November 1970.
2. Batchelor, G. K.; Application of the Similarity Theory of Turbulence to Atmospheric Diffusion, Quarterly Journal of the Royal Meteorological Society, 76 (328), pp. 133-146, 1950.
3. Calder, K. L.; "Some Miscellaneous Aspects of Current Urban Pollution Models" in Proceedings of Symposium on Multiple Source Urban Diffusion Models edited by A. C. Stern, U. S. Environmental Protection Agency, Air Pollution Control Office, Research Triangle Park, North Carolina, AP-86, 1970.
4. Desalu, A. A.; Dynamic Air Quality Estimation In A Stochastic Dispersive Atmosphere, Ph.D. Dissertation, the Department of Electrical Engineering, Massachusetts Institute of Technology, May 1974.
5. Friedman, E. and Ghovanlou, A.: Evaluation of Satellite Borne Air Pollution Remote Sensors, MTR-6783 for NASA Langley Research Center, Contract F-19628-75-C0001 by the Mitre Corporation, McLean Virginia 22101, November 1974.
6. Gifford, F.A., Jr.; Statistical Properties of a Fluctuating Plume Dispersion Model, Advances in Geophysics Vol. 6, Academic Press, 1959.
7. Gifford, F.A., Jr.; Peak to Average Concentration Ratios According to a Fluctuating Plume Dispersion Model, Intern. J. Air Pollution 3, pp. 253-260, 1960.
8. Gifford, F.A., Jr.; Use of Routine Meteorological Observations for Estimating Atmospheric Dispersion, Nuclear Safety, 2, 4, pp. 47-51, 1961.
9. Hamilton, P. M.; The Application of Pulsed-Light Rangefinder (LIDAR) to the Study of Chimney Plumes, Philosophical Transactions of the Royal Society of London, Series A, 265, pp. 153-172, 1969.
10. Heffter, J. L.; The Variation of Horizontal Diffusion Parameters with Time for Travel Periods of One Hour or Longer, Journal of Applied Meteorology, 4, pp. 153-156, 1965.

11. Hilst, G.R.; Observations of the Diffusion and Transport of Stack Effluents in Stable Atmospheres, Ph.D. Thesis, University of Chicago, 1957.
12. Hino, M.; Maximum Ground-Level Concentration and Sampling Time, Atmospheric Environment, 2, p. 149 ff, 1968.
13. Högström, U.; An Experimental Study on Atmospheric Diffusion, Tellus, 16, pp. 205-251, 1964.
14. Koch, R. C. and Fisher, G. E.; Evaluation of the Multiple-Source Gaussian Plume Diffusion Model, Report No. EF-186, for Environmental Protection Agency, Research Triangle Park, North Carolina by Geomet, Inc., Rockville, Maryland, April 1973.
15. Koch, R. C. and Thayer, S. D.; Validation and Sensitivity Analysis of the Gaussian Plume Multiple-Source Urban Diffusion Model, Report No. EF-60 for Environmental Protection Agency, Research Triangle Park, North Carolina by Geomet, Inc., Rockville, Maryland, November 1971.
16. McElroy, J. L. and Pooler, F., Jr.; St. Louis Dispersion Study, Vol. II: Analysis. National Air Pollution Control Administration, Raleigh, North Carolina, AP-53, 1968.
17. Papoulis, A.; Probability, Random Variables and Stochastic Processes, McGraw-Hill, New York, 1965.
18. Pasquill, F.; The Estimation of the Dispersion of Windborne Material, Meteorological Magazine, 90 (1063), pp. 33-49, 1961.
19. Pasquill, F.; Atmospheric Diffusion, D. Van Nostrand, Co., London, 1962.
20. Pasquill, F.; Atmospheric Diffusion, Second Edition, John Wiley & Sons, New York, 1974.
21. Pimental, K. D.; Toward a Mathematical Theory of Environmental Monitoring: The Infrequent Sampling Problem, Ph.D. Lissertation, The University of California at Livermore, June 1975.
22. Scorer, R. A.; Natural Aerodynamics, Pergamon Press, London, 1958.
23. Scorer, R. S.; Air Pollution, Pergamon Press, Oxford, 1968.
24. Slade, D. H.; Meteorology And Atomic Energy 1968, U. S. Atomic Energy Commission, Office of Information Services, 1968.

25. Smith, F. B.; (unpublished) reported in Gifford (1960) and F. Pasquill Atmospheric Diffusion (1974).
26. Smith, G. L., Green, R. N., and Young, G. R.; Statistical Interpretation of Pollution Data From Sattelites, presented at AIAA Mechanics and Control of Flight Conference, Anaheim, California, August 5-9, 1974 (1974a).
27. Smith, G. L., Green, R. N., and Young, G. R.; Interpretation of Air Pollution Data as Measured by an Airborne Remote Sensor, presented at Sixth Conference on Aerospace and Aeronautical Meteorology, El Paso, Texas, November 12-15, 1974 (1974b).
28. Turner, D. B.; Workbook of Atmospheric Dispersion Estimates, National Air Pollution Control Administration, Cincinnati, Ohio, AP-26, 1970.
29. Williamson, S. J.; Fundamentals of Air Pollution, Addison-Wesley, Reading, Mass., 1973.

APPENDIX A

DEVELOPMENT OF INSTANTANEOUS PLUME CENTERLINE MODEL

Let us consider the development of a functional form for $D_\eta(x,t)$, where the symbol $D_\eta(x,t)$ will be understood to refer to either $D_y(x,t)$ or $D_z(x,t)$. Similarly, D_η^2 will refer to either D_y^2 or D_z^2 . Let $\Sigma_\eta(x)$ denote the standard deviation of D_η ($\Sigma_\eta = \sqrt{D_\eta^2}$). The form of Σ_η will be given by the square root of expressions like equations (47), (50), or (58). The pertinent constraints for our model, however, appear to be that $\Sigma_\eta(0) = 0$, $\Sigma_\eta(x)$ is monotonically increasing, and $\Sigma_\eta(x)$ is bounded for $x > 0$.

We wish to find a function, $D_\eta(x,t)$ which describes the position (in η) of the instantaneous plume centerline. This function must, for fixed time, be oscillatory in x with increasing amplitude and wavelength. For fixed x , its time average must be zero and its standard deviation must be $\Sigma(x)$. It must additionally satisfy the properties that both its x and t correlations go to zero with increasing separation and that for fixed x the dominant behavior as time passes is that the upstream pattern drifts by at the mean wind speed.

The basic initial form was:

$$D_\eta(x,t) = f_\eta(x) \sin g_\eta(x,t). \quad (A1)$$

It is required that, for fixed t , the wavelength should bear some relation to the amplitude, i.e. if $g_\eta(x+\Delta, t) = g_\eta(x, t) + 2\pi$, then $\Delta = cf$. This constraint was implemented by letting

$$g_\eta(x,t) = \frac{2\pi}{c(f+\epsilon)} (x - \bar{U}t) , \quad (A2)$$

where \bar{U} is the mean wind speed and ϵ is a small positive number, used to prevent singularity at the origin. In practice, ϵ is approximately equal to the inner diameter of the stack or exit orifice. For fixed t , letting Δ be the effective wavelength,

$$2\pi = \frac{2\pi}{c} \left[\frac{x+\Delta-\bar{U}t}{f_{\eta}(x+\Delta)+\epsilon} - \frac{x-\bar{U}t}{f_{\eta}(x)+\epsilon} \right] \quad (A3)$$

It can be assumed that the change in amplitude (given by f_{η}) will be small over one wavelength (Δ) and therefore the approximation can be made that $\Delta = cf_{\eta}(x)$, which is the desired condition. The constant c is equal to 2π for a sinusoid, so that we will take $c \approx 6$.

The introduction of time dependence in the form $(x-\bar{U}t)$ is the standard procedure for guaranteeing that, as time passes, the upstream wave passes by.

$$D_{\eta}(x,t) = f_{\eta}(x) \sin \left[\frac{2\pi}{c(f_{\eta}+\epsilon)} (x-\bar{U}t) \right] \quad (A4)$$

is completely deterministic; for fixed x , the centerline is a sinusoid with fixed amplitude and wavelength. Some randomness must be introduced, however. A random (in time) additive phase angle is a simple way to provide this variation, but is not completely satisfactory in that the maximum amplitude for fixed x is constant, the x -correlation does not go to zero, and the distribution for fixed x is that of $\sin t$, i.e., the density function of $\frac{f_D}{f_{\eta}(x)}$ can be shown to be of the form:

$$\frac{f_D}{f_{\eta}}(\eta) = \frac{1}{\pi \sqrt{1-\eta^2}} \quad (A5)$$

where $\eta = y$ for D_y and $\eta = z$ for D_z .

In order to provide a random amplitude and at the same time given D a normal distribution, a multiplicative Gaussian process was introduced:

$$D_{\eta}(x,t) = f_{\eta}(x) \gamma_{1_{\eta}}(t) \sin \left[\frac{2\pi}{c(f_{\eta}+\epsilon)} (x-\bar{U}t) \right] \quad (A6)$$

where $\gamma_{1_{\eta}}(t)$ is a random process with density function:

$$f_{\gamma_{1_{\eta}}}(\eta) = \frac{\eta}{s_1^2} \exp \left\{ -\frac{\eta^2}{2s_1^2} \right\}, \quad \eta > 0 \quad (A7)$$

γ_1 has the properties $E\gamma_1 = \sqrt{\pi/2} s_1$; $E\gamma_1^2 = 2s_1^2$; Mode = s_1 ; Median = $1.1774s_1$; $E(\gamma_1 - \sqrt{\pi/2} s_1)^2 = \frac{4-\pi}{2} s_1^2$. It can then be shown that the variance of $D_\eta(x, t)$ for fixed x is $D_\eta^2 = f_\eta^2(x) s_1^2$.

Now consider

$$E(D_\eta(x, t) D_\eta(x, t+\tau)) = f_\eta^2(x) E\left(\gamma_{1_\eta}(t) \gamma_{1_\eta}(t+\tau) \sin\left[\frac{2\pi}{c(f_\eta + \epsilon)} (x - \bar{U}t)\right] \times \sin\left[\frac{2\pi}{c(f_\eta + \epsilon)} (x - \bar{U}t - \bar{U}\tau)\right]\right) \quad (A8)$$

This depends upon the correlation time of γ_1 , but will never go to zero because $E\gamma_1 \approx 1.25s_1 > 0$. Thus, a second random variable γ_{2_η} is required in the representation, with frequency function

$$f_{\gamma_{2_\eta}}(\eta) = \frac{\eta}{s_2^2} \exp\left\{-\frac{\eta^2}{2s_2^2}\right\}, \quad \eta > 0 \quad (A9)$$

Then:

$$D_\eta(x, t) = f_\eta(x) \gamma_{1_\eta}(t) \sin\left[\frac{2\pi}{c(f_\eta + \epsilon)} \gamma_{2_\eta}(t) (x - \bar{U}t)\right] \quad (A10)$$

γ_{2_η} has the property of modulating the frequency in a random fashion, thus making the correlation of D_η go to zero (in both x and t) as the separation goes to infinity. Consider first:

$$E(D_\eta(x, t) D_\eta(x+\Delta, t)) = f_\eta(x) f_\eta(x+\Delta) E(\gamma_{1_\eta}^2(t)) E(\sin[\omega_\eta(x) \gamma_{2_\eta}(x - \bar{U}t)] \sin[\omega_\eta(x+\Delta) \gamma_{2_\eta}(x - \bar{U}t + \Delta)]), \quad (A11)$$

where the expectation operator can be distributed because of independence and $\omega_\eta(x) = \frac{2\pi}{c(\epsilon + f_\eta(x))}$. It can be shown that

$$\lim_{\Delta \rightarrow \infty} E(\sin[\omega_\eta(x) \gamma_{2_\eta}(t) (x - \bar{U}t)] \sin[\omega_\eta(x+\Delta) \gamma_{2_\eta}(t) (x - \bar{U}t + \Delta)]) = 0 \quad (A12)$$

and that

$$\lim_{\tau \rightarrow \infty} E(D_\eta(x, t) D_\eta(x, t+\tau)) = \lim_{\tau \rightarrow \infty} f_\eta^2(x) E(\gamma_{1_\eta}(t) \gamma_{1_\eta}(t+\tau)) E(\sin[\omega_\eta \gamma_{2_\eta}(t) (x - \bar{U}t)] \sin[\omega_\eta \gamma_{2_\eta}(t+\tau) (x - \bar{U}t - \bar{U}\tau)]) = 0 \quad (A13)$$

Because γ_2 , as well as γ_1 , should have small probability of being zero (in order to prevent the identical vanishing of $D_\eta(x,t)$), the same distribution has been used for both $\gamma_{1\eta}$ and $\gamma_{2\eta}$, i.e.:

$$\left. \begin{aligned} \gamma_{1\eta} &= \sqrt{u_{1\eta}^2 + u_{2\eta}^2} \\ \gamma_{2\eta} &= \sqrt{u_{3\eta}^2 + u_{4\eta}^2} \end{aligned} \right\} \quad (A14)$$

where u_i ($i=1,2,3,4$) are Gaussian random variables. The $u_{i\eta}$ can be generated as the output of linear systems driven by white noise,

$$\dot{u}_{i\eta} = -\mu_{i\eta} u_{i\eta} + v_{i\eta}, \quad i = 1,2,3,4 \quad (A15)$$

where $E v_{i\eta} = 0$, $E(v_{i\eta}(t) v_{i\eta}(t+\tau)) = q_{i\eta} \delta(\tau)$, and where $\delta(\tau)$ is the Dirac delta function, and it is well known that:

$$E(u_{i\eta}(t) u_{i\eta}(t+\tau)) = \frac{q_{i\eta}}{2\mu_{i\eta}} e^{-\mu_{i\eta} |\tau|}, \quad i = 1,2,3,4 \quad (A16)$$

Unfortunately the density function for $\gamma_{1\eta}$ has only one free parameter, s_1 . Thus we are forced to accept whatever variations in peak amplitude are implied by obtaining the desired variance of D_η . Thus if we take $s_1 = 1$ and let $f_\eta(x) = \Sigma_\eta(x)$, we find that the mode peak is Σ_η , the mean peak is $\frac{\pi}{2} \Sigma_\eta \approx 1.25 \Sigma_\eta$ and the variance in peak amplitude is $E(\Sigma_\eta(x) \gamma_{1\eta} - \sqrt{\frac{\pi}{2}} \Sigma_\eta)^2 = \frac{4-\pi}{2} \Sigma_\eta^2 \approx 0.43 \Sigma_\eta^2$.

For the correlation of $\gamma_{1\eta}(t)$, we would like to have a time of perhaps one period of the asymptotic waves, i.e. $T_\eta = \frac{cf_\eta(\infty)}{U}$. This is probably too long a memory near the stack, however this constancy is a consequence of the model. Also we let this be the correlation of $u_{1\eta}$ and $u_{2\eta}$ rather than $\gamma_{1\eta}$, so

$$\left. \begin{aligned} \dot{u}_{1\eta} &= -\frac{1}{T_\eta} u_{1\eta} + v_{1\eta} \\ \dot{u}_{2\eta} &= -\frac{1}{T_\eta} u_{2\eta} + v_{2\eta} \end{aligned} \right\} \quad , \quad (A17)$$

where it follows from (A16) that $q_{1\eta} = q_{2\eta} = \frac{2}{T_\eta} s_1^2 = \frac{2}{T_\eta}$, $T_\eta = \frac{cf_\eta(\infty)}{U}$.

The statistics of γ_{2_n} are selected so that mean amplitude and mean wavelength are in the ratio c . This requires that $s_2 = \frac{2}{\pi}$. The correlation time of γ_{2_n} can be taken the same as that of γ_{1_n} so that

$$\left. \begin{aligned} \dot{u}_{3_n} &= -\frac{1}{T_n} u_{3_n} + v_{3_n} \\ \dot{u}_{4_n} &= -\frac{1}{T_n} u_{4_n} + v_{4_n} \end{aligned} \right\} \quad (A18)$$

where $q_{3_n} = q_{4_n} = \frac{2}{T_n} s_2^2 = \frac{8}{T_n \pi^2}$.

The frequency functions for D_n are now Gaussian, as required:

$$f_{D_n}(\eta) = [2\pi \overline{D_n^2}]^{-\frac{1}{2}} \exp \{ -\eta^2 / 2\overline{D_n^2} \} \quad (A19)$$

where

$$f_{D_y}(y) = g_1(D_y), \quad f_{D_z}(z) = g_2(D_z) \quad \text{in the notation of Section III.}$$

APPENDIX B

CONSIDERATIONS OF THE GAUSSIAN NATURE OF PLUME PARAMETERS

The purpose of this appendix is to consider, from several different approaches, the question of Gaussian distributions appearing in the plume. We might call attention to the concept that the material distribution of a cloud (large number of samples) of particles, each of which is a random variable, should approximate a scalar multiple of the frequency function (Law of Large Numbers).

1) The usual beginning model for diffusion is the heat equation:

$$\frac{\partial X}{\partial t} = \frac{\partial^2 X}{\partial y^2} . \quad (B1)$$

This has the solution:

$$X = Q e^{-\frac{y^2}{t}} , \quad (B2)$$

which is a Gaussian waveform having variance increasing linearly with time.

2) Another approach to diffusion is stochastic, with Brownian motion as the motivating physics. In this case we have a single particle being forced by a random process,

$$\dot{x}(t) = u(t) . \quad (B3)$$

We assume that there is no homogeneous restoring force (isotropy), so the motion is described as pure integration of u . Under very weak restrictions on u , the probability distribution of $x(t)$ is asymptotically Gaussian (with t). It should be noted that if u is Gaussian white noise, then $x(t)$ is normally distributed for all t , provided that the initial distribution is normal. These results essentially follow from the Central Limit Theorem. To complete the connection with the diffusion equation, if the particle starts at the origin and u is Gaussian white noise, then the variance of x is linear with time.

Consider a single particle of pollutant. Its position at some time after release from the source is determined as the sum of all incremental perturbations during the elapsed time. This corresponds to a random walk or Brownian motion.

Under these circumstances, the distribution of the particle at some later time is normal. Using the Law of Large Numbers, the material distribution of a large number of pollutant particles (the average plume) can be expected to approximate a scalar multiple of the frequency function, i.e. should be Gaussian. Actually this argument seems to suggest that each plume realization, which involves a large number of particles, should approximate the frequency function precisely because it is an ensemble average over a large number of individual particle realizations. This argument breaks down, however, because of the high correlation of the low frequency forcing terms (medium to large scale eddies) appearing in this single plume realization. These low frequency terms require long averaging times to reduce the effects of their long correlation times.

3) Closely allied to the random walk in (2) is the system:

$$\dot{x}(t) = a \cos t + b \sin t \quad (B4)$$

where a and b are independent normally distributed random variables, and we consider the ensemble of random variables $\{x(t)\}$; these are normally distributed. Actually, this fact has been used already in A6 and A7.

There are two generalizations of this result. In one, we can allow a and b to be stochastic variables with time constants long with respect to the sinusoid frequency. In the other, we suppose \dot{x} to be a sum of such terms,

$$\dot{x} = \sum_{k=1}^N a_k \cos \omega_k t + b_k \sin \omega_k t \quad (B5)$$

Assuming the sinusoids to be independent over the region of interest, then the distribution of $x(t)$ will be asymptotically (with increasing N) normal, regardless of the distribution of the coefficients. This is a consequence of (2) and the Central Limit Theorem.

We have examined this particular model, because it corresponds in some intuitive way to pollutant forcing terms, the eddies being sinusoids of essentially random amplitude, phase, and frequency. Under these circumstances we can see: the average plume is expected to be Gaussian; any bandpass of the solution is expected to be Gaussian - hence both D_y and the distribution in the instantaneous plume are Gaussian; and finally, the averaging time required to pick up several realizations becomes long as the scale of the eddies increases.

4) In Section III, we have argued that the distribution of material in the instantaneous plume described by $f(y - D_y, t; y_0, t_0)$ is gaussian. This result was obtained by voting that if equation (5) holds and both $E(-\frac{x}{Q_d})$ and $g(D_y)$ are gaussian, then f must be gaussian. The inversion of the integral equation (equation (5)) is poorly conditioned, however, and many different distribution will be mapped by (5) into approximately gaussian forms.

Thus our objection can be raised to the conclusion that f is gaussian. For modeling purposes, however, there is nothing inconsistent about defining f to be gaussian since this agrees with observations and also satisfies our feeling that, from the Central Limit Theorem, the frequency function for particles about the instantaneous center line should be gaussian.